
The Reflectron: Exploiting geometry for learning generalized linear models

Nicholas M. Boffi

Paulson School of Engineering and Applied Sciences
Harvard University
Cambridge, MA 02138
boffi@g.harvard.edu

Jean-Jacques E. Slotine

Nonlinear Systems Laboratory
Massachusetts Institute of Technology
Cambridge, MA 02139
jjs@mit.edu

Abstract

Generalized linear models (GLMs) extend linear regression by generating the dependent variables through a nonlinear function of a predictor in a Reproducing Kernel Hilbert Space. Despite nonconvexity of the underlying optimization problem, the GLM-tron algorithm of Kakade et al. (2011) provably learns GLMs with guarantees of computational and statistical efficiency. We present an extension of the GLM-tron to a mirror descent or natural gradient-like setting, which we call the Reflectron. The Reflectron enjoys the same statistical guarantees as the GLM-tron for any choice of the convex potential function ψ used to define mirror descent. Central to our algorithm, ψ can be chosen to implicitly regularize the learned model when there are multiple hypotheses consistent with the data. Our results extend to the case of multiple outputs with or without weight sharing. We perform our analysis in continuous-time, leading to simple and intuitive derivations, with discrete-time implementations obtained by discretization of the continuous-time dynamics. We supplement our theoretical analysis with simulations on real and synthetic datasets demonstrating the validity of our theoretical results.

1 Introduction

Generalized linear models (GLMs) represent a powerful extension of linear regression. In a GLM, the dependent variables y_i are assumed to be given as a known nonlinear “link” function u of a linear predictor of the covariates, $\mathbb{E}[y_i|\mathbf{x}_i] = u(\mathbf{w}^T \mathbf{x}_i)$, for some fixed vector of parameters \mathbf{w} . GLMs are readily kernelizable, which captures the more flexible setting $\mathbb{E}[y_i|\mathbf{x}_i] = u(\langle \boldsymbol{\alpha}(\mathbf{x}_i), \mathbf{w} \rangle)$ where $\boldsymbol{\alpha}(\cdot)$ is a feature map in a Reproducing Kernel Hilbert Space (RKHS) and $\langle \cdot, \cdot \rangle$ denotes the RKHS inner product. A prominent example of a GLM that arises in practice is logistic regression, which has wide-reaching applications in the natural, social, and medical sciences (Sur and Candès, 2019). Similarly, an immediate example of a kernel-based GLM is kernel logistic regression. Extensive details on GLMs can be found in the standard reference (McCullagh and Nelder, 1989).

The GLM-tron of Kakade et al. (2011) is the first computationally and statistically efficient algorithm for learning GLMs. Inspired by the Isotron of Kalai and Sastry (2009), it is a simple and intuitive Perceptron-like algorithm applicable for learning arbitrary GLMs with a nondecreasing and Lipschitz link function. In this work, we revisit the GLM-tron from a new perspective, leveraging recent developments continuous-time optimization and adaptive control theory (Boffi and Slotine, 2019). We consider the continuous-time limit of the GLM-tron, and generalize the resulting continuous-time dynamics to a mirror descent-like (Beck and Teboulle, 2003; Krichene et al., 2015) setting, which we call the Reflectron. By their equivalence in continuous-time, our analysis also applies to natural gradient variants of the GLM-tron (Amari, 1998; Pascanu and Bengio, 2013). We prove non-asymptotic generalization error bounds for the resulting family of continuous-time dynamics –

parameterized by the choice of potential function ψ – and we further prove convergence rates in the realizable setting. Our continuous-time Reflectron immediately gives rise to a wealth of discrete-time algorithms by choice of discretization method, allowing us to leverage the vast body of work in numerical analysis (Butcher, 2001) and the widespread availability of off-the-shelf black-box ordinary differential equation solvers.

We connect the Reflectron algorithm with the growing body of literature on the implicit bias of optimization algorithms by applying a recent continuous-time limit (Boffi and Slotine, 2019) of a simple proof methodology for analyzing the implicit regularization of stochastic mirror descent (Azizan et al., 2019; Azizan and Hassibi, 2019). We show that, in the realizable setting, the choice of potential function ψ implicitly biases the learned parameters to minimize ψ . We extend our results to a vector-valued setting which allows for weight sharing between output components, extending the Euclidean variant with independent weights first considered by Foster et al. (2020). We prove that convergence, implicit regularization, and similar generalization error bounds hold in this setting.

1.1 Related work and significance

The GLM-tron has recently seen impressive applications in both statistical learning and learning-based control theory. The original work applied the GLM-tron to efficiently learn Single Index Models (SIMs) (Kakade et al., 2011). A recent extension (the BregmanTron) uses Bregman divergences to obtain improved guarantees for learning SIMs, though their use of Bregman divergences is different from ours (Nock and Menon, 2020). Foster et al. (2020) utilized the GLM-tron to develop an adaptive control law for stochastic, nonlinear, and discrete-time dynamical systems. Goel and Klivans (2017) use the kernelized GLM-tron, the Alphasatron, to provably learn two hidden layer neural networks, while Goel et al. (2018) generalize the Alphasatron to the Convotron for provable learning of one hidden layer convolutional neural networks. Orthogonally, but much like (Foster et al., 2020), GLM-tron-like update laws have been developed in the adaptive control literature (Tyukin et al., 2007), along with mirror descent and momentum-like variants (Boffi and Slotine, 2019), where they can be used for provable control of unknown and nonlinearly parameterized dynamical systems. Our work extends this line of research by allowing for the incorporation of local geometry into the GLM-tron update for regularization of the learned parameters.

Similarly, continuous-time approaches in machine learning and optimization have become increasingly fruitful tools for analysis. Su et al. (2016) derive a continuous-time limit of Nesterov’s celebrated accelerated gradient method (Nesterov, 1983), and show that this limit enables intuitive proofs via Lyapunov stability theory. Krichene et al. (2015) perform a similar analysis for mirror descent, while Zhang et al. (2018) show that using standard Runge-Kutta integrators on the second-order dynamics of Su et al. (2016) preserves acceleration. Lee et al. (2016) show via dynamical systems theory that saddle points are almost surely avoided by gradient descent with a random initialization. Boffi and Slotine (2020) use a continuous-time view of distributed stochastic gradient descent methods to analyze the effect of distributed coupling on SGD noise. Remarkably, Wibisono et al. (2016), Betancourt et al. (2018), and Wilson et al. (2016) show that many accelerated optimization algorithms can be generated by discretizing the Euler-Lagrange equations of a certain functional known as the Bregman Lagrangian. For deep learning, Chen et al. (2018) show that residual networks can be interpreted as a forward-Euler discretization of a continuous-time dynamical system, and use higher-order integrators to arrive at alternative architectures. Our work continues in this promising line of recent work, and highlights that continuous-time offers clean and intuitive proofs that can later be discretized for guarantees on discrete-time algorithms.

As exemplified by the field of deep learning, modern machine learning frequently takes place in a high-dimensional regime with more parameters than examples. It is now well-known that deep networks will interpolate noisy data, yet exhibit low generalization error *despite interpolation* when trained on meaningful data (Zhang et al., 2016). Defying classical statistical wisdom, an explanation for this apparent paradox has been given in the *implicit bias* of optimization algorithms and the double-descent curve (Belkin et al., 2019a). The notion of implicit bias captures the preference of an optimization algorithm to converge to a particular kind of interpolating solution – such as a minimum norm solution – when many options exist. Surprisingly, similar “harmless” or “benign” interpolation phenomena have been observed even in much simpler systems such as overparameterized linear regression (Bartlett et al., 2019; Muthukumar et al., 2019; Hastie et al., 2019) and random feature

models (Belkin et al., 2019b; Mei and Montanari, 2019). Understanding implicit bias has thus become an important area of research, with applications ranging from modern deep learning to pure statistics.

Implicit bias has been categorized for separable classification problems (Soudry et al., 2018; Nacson et al., 2018), regression problems using mirror descent (Gunasekar et al., 2018b), and multilayer models (Gunasekar et al., 2018a; Woodworth et al., 2020; Gunasekar et al., 2017). Approximate results and empirical evidence are also available for nonlinear deep networks (Azizan et al., 2019). Our work contributes to the understanding of implicit bias in a practically relevant class of nonconvex learning problems, where proofs of convergence and bounds on the generalization error are attainable: GLM regression. Our algorithms have applications in recovering the weights of an unknown recurrent neural network, and may be useful for learning single-layer neural network models (Bai et al., 2019).

2 Problem setting and background

Our setup follows the original work of Kakade et al. (2011). We assume the dataset $\{\mathbf{x}_i, y_i\}_{i=1}^m$ is sampled i.i.d. from a distribution \mathcal{D} supported on $\mathcal{X} \times [0, 1]$, where $\mathbb{E}[y_i|\mathbf{x}_i] = u(\langle \boldsymbol{\alpha}(\mathbf{x}_i), \boldsymbol{\theta} \rangle)$ for $\boldsymbol{\alpha}(\mathbf{x}) \in \mathbb{R}^p$ a finite-dimensional feature map with associated kernel $\mathcal{K}(\mathbf{x}_1, \mathbf{x}_2) = \langle \boldsymbol{\alpha}(\mathbf{x}_1), \boldsymbol{\alpha}(\mathbf{x}_2) \rangle$ and $\boldsymbol{\theta} \in \mathbb{R}^p$ a fixed, unknown vector of parameters. $u : \mathbb{R} \rightarrow [0, 1]$ is a known, nondecreasing, and L -Lipschitz link function. We assume that $\|\boldsymbol{\theta}\| \leq W$ for some fixed bound W and that $\|\boldsymbol{\alpha}(\mathbf{x})\| \leq C$ for all $\mathbf{x} \in \mathcal{X}$ for some fixed bound C . Our goal is to approximate $\mathbb{E}[y_i|\mathbf{x}_i]$ as measured by the expected squared loss. To this end, for a hypothesis $h(\cdot)$ we define the quantities

$$\text{err}(h) = \mathbb{E}_{\mathbf{x}, y} \left[(h(\mathbf{x}) - y)^2 \right], \quad (1)$$

$$\varepsilon(h) = \text{err}(h) - \text{err}(\mathbb{E}[y|\mathbf{x}]) = \mathbb{E}_{\mathbf{x}, y} \left[(h(\mathbf{x}) - u(\langle \boldsymbol{\alpha}(\mathbf{x}), \boldsymbol{\theta} \rangle))^2 \right], \quad (2)$$

and we denote their empirical counterparts over the dataset as $\widehat{\text{err}}(h)$ and $\widehat{\varepsilon}(h)$. Above, $\text{err}(h)$ measures the generalization error of $h(\cdot)$, while ε measures the excess risk compared to the Bayes-optimal predictor. Towards minimizing $\text{err}(h)$, we present a family of mirror descent-like algorithms for minimizing $\widehat{\varepsilon}(h)$ over parametric hypotheses of the form $h(\mathbf{x}) = u(\langle \boldsymbol{\alpha}(\mathbf{x}), \hat{\boldsymbol{\theta}} \rangle)$. Via standard statistical bounds (Bartlett and Mendelson, 2002), we transfer our guarantees on $\widehat{\varepsilon}(h)$ to $\varepsilon(h)$, which in turn implies a small $\text{err}(h)$. The starting point of our analysis is the GLM-tron of Kakade et al. (2011). The GLM-tron is an iterative update law of the form

$$\hat{\boldsymbol{\theta}}_{t+1} = \hat{\boldsymbol{\theta}}_t - \frac{1}{m} \sum_{i=1}^m \left(u(\langle \boldsymbol{\alpha}(\mathbf{x}_i), \hat{\boldsymbol{\theta}} \rangle) - y_i \right) \boldsymbol{\alpha}(\mathbf{x}_i) \quad (3)$$

with initialization $\hat{\boldsymbol{\theta}}_0 = \mathbf{0}$. (3) is a gradient-like update law, obtained from gradient descent on the square loss $\widehat{\text{err}}(h)$ by dropping the derivative of u . It admits a natural continuous-time limit,

$$\frac{d}{dt} \hat{\boldsymbol{\theta}} = -\frac{1}{m} \sum_{i=1}^m \left(u(\langle \boldsymbol{\alpha}(\mathbf{x}_i), \hat{\boldsymbol{\theta}} \rangle) - y_i \right) \boldsymbol{\alpha}(\mathbf{x}_i) \quad (4)$$

where (4) is obtained from (3) via a forward-Euler discretization with a timestep $\Delta t = 1$. Throughout this paper, we will use the notation $\frac{d}{dt} \mathbf{x} = \dot{\mathbf{x}}$ interchangeably for any time-dependent signal $\mathbf{x}(t)$.

3 The Reflectron Algorithm

We define the Reflectron algorithm in continuous-time as the mirror descent-like dynamics

$$\frac{d}{dt} \nabla \psi(\hat{\boldsymbol{\theta}}) = -\frac{1}{m} \sum_{i=1}^m \left(u(\langle \boldsymbol{\alpha}(\mathbf{x}_i), \hat{\boldsymbol{\theta}} \rangle) - y_i \right) \boldsymbol{\alpha}(\mathbf{x}_i) \quad (5)$$

for ψ a convex function. The parameters of the hypothesis h_t at time t are obtained by applying the inverse gradient of ψ to the output of the Reflectron.

3.1 Statistical guarantees

The following theorem gives our statistical guarantees for the Reflectron. It implies that for any choice of strongly convex function ψ , the Reflectron finds a nearly Bayes-optimal predictor if it is allowed to run for sufficiently long time.

Theorem 3.1 (Statistical guarantees for the Reflectron). *Suppose that $\{\mathbf{x}_i, y_i\}_{i=1}^m$ are drawn i.i.d. from a distribution \mathcal{D} supported on $\mathcal{X} \times [0, 1]$ with $\mathbb{E}[y|\mathbf{x}] = u(\langle \boldsymbol{\theta}, \boldsymbol{\alpha}(\mathbf{x}) \rangle)$ for a known nondecreasing and L -Lipschitz link function $u : \mathbb{R} \rightarrow [0, 1]$, a kernel function \mathcal{K} with corresponding finite-dimensional feature map $\boldsymbol{\alpha}(\mathbf{x}) \in \mathbb{R}^p$, and an unknown vector of parameters $\boldsymbol{\theta} \in \mathbb{R}^p$. Assume that $d_\psi(\boldsymbol{\theta} \parallel \mathbf{0}) \leq \frac{\sigma}{2}W^2$ where ψ is σ -strongly convex with respect to $\|\cdot\|_2$ and $W > 0$ is a constant, and that $\|\boldsymbol{\alpha}(\mathbf{x})\| \leq C$ for all $\mathbf{x} \in \mathcal{X}$ where $C > 0$ is a constant. Then, for any $\delta \in (0, 1)$, with probability at least $1 - \delta$ over the draws of the $\{\mathbf{x}_i, y_i\}$, there exists some time $t < \mathcal{O}\left(\frac{\sigma W}{C} \sqrt{m/\log(\frac{1}{\delta})}\right)$ such that the hypothesis $h_t = u(\langle \hat{\boldsymbol{\theta}}(t), \boldsymbol{\alpha}(\mathbf{x}) \rangle)$ satisfies*

$$\max\{\widehat{\varepsilon}(h_t), \varepsilon(h_t)\} \leq \mathcal{O}\left(LCW \sqrt{\frac{\log(1/\delta)}{m}}\right),$$

where $\hat{\boldsymbol{\theta}}(t)$ is output by the Reflectron at time t with $\hat{\boldsymbol{\theta}}(0) = \mathbf{0}$.

Proof. Consider the rate of change of the Bregman divergence (Bregman, 1967)

$$d_\psi(\boldsymbol{\theta}_1 \parallel \boldsymbol{\theta}_2) = \psi(\boldsymbol{\theta}_1) - \psi(\boldsymbol{\theta}_2) - \langle \nabla \psi(\boldsymbol{\theta}_2), \boldsymbol{\theta}_1 - \boldsymbol{\theta}_2 \rangle$$

between the parameters for the Bayes-optimal predictor and $\hat{\boldsymbol{\theta}}(t)$, $\frac{d}{dt}d_\psi(\boldsymbol{\theta} \parallel \hat{\boldsymbol{\theta}}) = \langle \hat{\boldsymbol{\theta}} - \boldsymbol{\theta}, \nabla^2 \psi(\hat{\boldsymbol{\theta}}) \hat{\boldsymbol{\theta}} \rangle$. Note that we have the equality $\frac{d}{dt} \nabla \psi(\hat{\boldsymbol{\theta}}) = \nabla^2 \psi(\hat{\boldsymbol{\theta}}) \hat{\boldsymbol{\theta}}$, and hence we find that

$$\begin{aligned} \frac{d}{dt}d_\psi(\boldsymbol{\theta} \parallel \hat{\boldsymbol{\theta}}) &= \frac{1}{m} \sum_{i=1}^m \left(u(\langle \boldsymbol{\alpha}(\mathbf{x}_i), \boldsymbol{\theta} \rangle) - u(\langle \boldsymbol{\alpha}(\mathbf{x}_i), \hat{\boldsymbol{\theta}} \rangle) \right) \langle \boldsymbol{\alpha}(\mathbf{x}_i), \hat{\boldsymbol{\theta}} - \boldsymbol{\theta} \rangle \\ &\quad + \frac{1}{m} \sum_{i=1}^m (y_i - u(\langle \boldsymbol{\alpha}(\mathbf{x}_i), \boldsymbol{\theta} \rangle)) \langle \boldsymbol{\alpha}(\mathbf{x}_i), \hat{\boldsymbol{\theta}} - \boldsymbol{\theta} \rangle. \end{aligned}$$

Using that u is L -Lipschitz and nondecreasing,

$$\frac{d}{dt}d_\psi(\boldsymbol{\theta} \parallel \hat{\boldsymbol{\theta}}) \leq -\frac{1}{L}\widehat{\varepsilon}(h_t) + \frac{1}{m} \sum_{i=1}^m (y_i - u(\langle \boldsymbol{\alpha}(\mathbf{x}_i), \boldsymbol{\theta} \rangle)) \langle \boldsymbol{\alpha}(\mathbf{x}_i), \hat{\boldsymbol{\theta}} - \boldsymbol{\theta} \rangle \quad (6)$$

Now, note that each $\frac{1}{C}(y_i - u(\langle \boldsymbol{\alpha}(\mathbf{x}_i), \boldsymbol{\theta} \rangle))\boldsymbol{\alpha}(\mathbf{x}_i)$ is a zero-mean i.i.d. random variable with norm bounded by 1 almost surely. Then, by Lemma C.1, $\|\frac{1}{Cm} \sum_{i=1}^m (y_i - u(\langle \boldsymbol{\alpha}(\mathbf{x}_i), \boldsymbol{\theta} \rangle))\boldsymbol{\alpha}(\mathbf{x}_i)\| \leq \eta$ with probability at least $1 - \delta$ where $\eta = \frac{2(1+\sqrt{\log(1/\delta)/2})}{\sqrt{m}}$. Assuming that $\|\hat{\boldsymbol{\theta}}(t) - \boldsymbol{\theta}\| \leq W$ at time t , we conclude that

$$\frac{d}{dt}d_\psi(\boldsymbol{\theta} \parallel \hat{\boldsymbol{\theta}}) \leq -\frac{1}{L}\widehat{\varepsilon}(h_t) + CW\eta.$$

Hence, either $\frac{d}{dt}d_\psi(\boldsymbol{\theta} \parallel \hat{\boldsymbol{\theta}}) < -CW\eta$, or $\widehat{\varepsilon}(h_t) \leq 2LCW\eta$. In the latter case, our result is proven.

In the former, by our assumptions $d_\psi(\boldsymbol{\theta} \parallel \mathbf{0}) = d_\psi(\boldsymbol{\theta} \parallel \hat{\boldsymbol{\theta}}(0)) \leq \frac{\sigma}{2}W^2$, and hence $\|\hat{\boldsymbol{\theta}}(0) - \boldsymbol{\theta}\| \leq W$

by σ -strong convexity of ψ with respect to $\|\cdot\|_2$. Furthermore, $\|\hat{\boldsymbol{\theta}}(t) - \boldsymbol{\theta}\| \leq \sqrt{\frac{2}{\sigma}d_\psi(\boldsymbol{\theta} \parallel \hat{\boldsymbol{\theta}}(t))} \leq$

$\sqrt{\frac{2}{\sigma}d_\psi(\boldsymbol{\theta} \parallel \hat{\boldsymbol{\theta}}(0))} \leq W$. Thus it can be until at most $t_f = \frac{d_\psi(\boldsymbol{\theta} \parallel \hat{\boldsymbol{\theta}}(0))}{CW\eta} = \frac{\sigma/2W^2}{CW\eta} = \frac{\sigma W}{2C\eta}$ to satisfy

$\widehat{\varepsilon}(h_t) \leq 2LCW\eta$. Hence there is some h_t with $t < t_f$ such that $\widehat{\varepsilon}(h_t) \leq \mathcal{O}\left(LCW \sqrt{\frac{\log(1/\delta)}{m}}\right)$.

To transfer this bound on $\widehat{\varepsilon}$ to ε , we need to bound the quantity $|\widehat{\varepsilon}(h_t) - \varepsilon(h_t)|$. Combining Theorems C.1 and C.2 gives us a bound on the Rademacher complexity $\mathcal{R}_m(\mathcal{F}) \leq \mathcal{O}\left(LCW\sqrt{\frac{1}{m}}\right)$ where $\mathcal{F} = \{u(\langle \mathbf{w}, \alpha(\mathbf{x}) \rangle) : \mathbf{x} \in \mathcal{X}, \|\mathbf{w}\| \leq 2W, \|\alpha(\mathbf{x})\| \leq C\}$, and clearly $h_t \in \mathcal{F}$. Application of Theorem C.3 to the square loss¹ immediately implies $|\widehat{\varepsilon}(h_t) - \varepsilon(h_t)| \leq \mathcal{O}\left(\frac{LCW}{\sqrt{m}}\right) + \mathcal{O}\left(\sqrt{\frac{\log(1/\delta)}{m}}\right)$ with probability at least $1 - \delta$. The conclusion of the theorem follows by a union bound. \square

Because $\varepsilon(h_t) = \text{err}(h_t)$ up to a constant, we can find a good predictor h_t by using a hold-out set to estimate $\text{err}(h_t)$ and by taking the best predictor on the hold-out set. Our proof of Theorem 3.1 is similar to the corresponding proofs of the GLM-tron (Kakade et al., 2011) and the Alphasatron (Goel and Klivans, 2017), but has two primary modifications. First, we consider the Bregman divergence under ψ between the Bayes-optimal parameters and the current parameters output by the Reflectron rather than the squared Euclidean distance. Second, rather than analyzing the *iteration* on $\|\widehat{\boldsymbol{\theta}}_t - \boldsymbol{\theta}\|^2$ as in the discrete-time case, we analyze the *time derivative* of the Bregman divergence. Taking $\psi = \frac{1}{2}\|\cdot\|^2$ recovers the guarantees of the Alphasatron², and taking $\alpha(\mathbf{x}) = \mathbf{x}$ recovers the guarantees of the GLM-tron, up to forward Euler discretization-specific details. As our analysis applies in the continuous-time setting, many algorithmic variants may be obtained by choice of discretization method. Because the Reflectron operates directly on $\widehat{\boldsymbol{\theta}}$ rather than $\widehat{\mathbf{c}}$ where $\langle \alpha(\mathbf{x}), \widehat{\boldsymbol{\theta}} \rangle = \sum_k \mathcal{K}(\mathbf{x}, \mathbf{x}_k) \widehat{c}_k$, we require the feature map to be finite-dimensional.

3.2 Implicit regularization

We now consider an alternative setting, and probe how the choice of ψ impacts the parameters learned by the Reflectron. We require the following assumption.

Assumption 3.1. The dataset $\{\mathbf{x}_i, y_i\}_{i=1}^m$ is realizable. That is, there exists some fixed parameter vector $\boldsymbol{\theta} \in \mathbb{R}^p$ such that $y_i = u(\langle \boldsymbol{\theta}, \alpha(\mathbf{x}_i) \rangle)$ for all i .

Assumption 3.1 allows us to understand both overfitting and interpolation by the Reflectron. In many cases, even the noisy dataset of Section 3.1 may satisfy Assumption 3.1. We begin by proving convergence of the Reflectron in the realizable setting.

Lemma 3.1 (Convergence of the Reflectron for a realizable dataset). *Suppose that $\{\mathbf{x}_i, y_i\}_{i=1}^m$ are drawn i.i.d. from a distribution \mathcal{D} supported on $\mathcal{X} \times [0, 1]$ and that Assumption 3.1 is satisfied where u is a known, nondecreasing, and L -Lipschitz function. Let ψ be any convex function with invertible Hessian over the trajectory $\widehat{\boldsymbol{\theta}}(t)$. Then $\widehat{\varepsilon}(h_t) \rightarrow 0$ where $h_t(\mathbf{x}) = u(\langle \widehat{\boldsymbol{\theta}}(t), \alpha(\mathbf{x}) \rangle)$ is the hypothesis with parameters output by the Reflectron at time t with $\widehat{\boldsymbol{\theta}}(0)$ arbitrary. Furthermore, $\inf_{t' \in [0, t]} \{\widehat{\varepsilon}(h_{t'})\} \leq \mathcal{O}\left(\frac{1}{t}\right)$.*

Proof. Under the assumptions of the lemma, (6) shows that

$$\frac{d}{dt} d_\psi(\boldsymbol{\theta} \parallel \widehat{\boldsymbol{\theta}}) \leq -\frac{1}{L} \widehat{\varepsilon}(h_t) \leq 0.$$

Integrating both sides of the above gives the bound

$$\int_0^t \widehat{\varepsilon}(h_{t'}) dt' \leq L \left(d_\psi(\boldsymbol{\theta} \parallel \mathbf{0}) - d_\psi(\boldsymbol{\theta} \parallel \widehat{\boldsymbol{\theta}}(t)) \right) \leq L d_\psi(\boldsymbol{\theta} \parallel \mathbf{0}).$$

Explicit computation shows that $\frac{d}{dt} \widehat{\varepsilon}(h_t)$ is bounded, so that $\widehat{\varepsilon}(h_t)$ is uniformly continuous in t . By Barbalat's Lemma (Lemma C.2), this implies that $\widehat{\varepsilon} \rightarrow 0$ as $t \rightarrow \infty$.

Furthermore, this simple analysis immediately gives us a convergence rate. Indeed, one can write

$$\inf_{t' \in [0, t]} \{\widehat{\varepsilon}(h_{t'})\} t = \int_0^t \inf_{t' \in [0, t]} \{\widehat{\varepsilon}(h_{t'})\} dt' \leq \int_0^t \widehat{\varepsilon}(h_{t'}) dt' \leq L d_\psi(\boldsymbol{\theta} \parallel \mathbf{0}),$$

so that $\inf_{t' \in [0, t]} \{\widehat{\varepsilon}(h_{t'})\} \leq \frac{L d_\psi(\boldsymbol{\theta} \parallel \mathbf{0})}{t}$. \square

¹Note that while the square loss is not bounded or Lipschitz in general, it is both over the domain $[0, 1]$ with bound $b = 1$ and Lipschitz constant $L' = 1$

²Our setting corresponds to the case where $\boldsymbol{\xi} = \mathbf{0}$ in the notation of Goel and Klivans (2017)

Lemma 3.1 shows that the Reflectron will converge to an interpolating solution in the realizable setting and that the best hypothesis up to time t does so at an $\mathcal{O}\left(\frac{1}{t}\right)$ rate. It also implies that the Bregman divergence remains bounded, which in many cases implies boundedness of $\hat{\theta}$ itself. In turn, for a realizable dataset, the strong convexity requirement of Theorem 3.1 can be relaxed to a requirement that $\nabla^2 \psi(\cdot)$ remains invertible over the trajectory $\hat{\theta}(t)$. Note that Lemma 3.1 allows for arbitrary initialization, while Theorem 3.1 requires $\hat{\theta}(0) = \mathbf{0}$.

In general, there may be many possible vectors $\hat{\theta}$ consistent with the data. The following theorem provides insight into the parameters learned by the Reflectron.

Theorem 3.2 (Implicit regularization of the Reflectron). *Consider the setting of Lemma 3.1. Let $\mathcal{A} = \{\bar{\theta} : u(\langle \bar{\theta}, \alpha(\mathbf{x}_i) \rangle) = y_i, i = 1, \dots, m\}$ be the set of parameters that interpolate the data, and assume that $\hat{\theta}(t) \rightarrow \hat{\theta}_\infty \in \mathcal{A}$. Further assume that $u(\cdot)$ is invertible. Then $\hat{\theta}_\infty = \arg \min_{\bar{\theta} \in \mathcal{A}} d_\psi(\bar{\theta} \parallel \hat{\theta}(0))$. In particular, if $\hat{\theta}(0) = \arg \min_{\mathbf{w} \in \mathbb{R}^d} \psi(\mathbf{w})$, then $\hat{\theta}_\infty = \arg \min_{\bar{\theta} \in \mathcal{A}} \psi(\mathbf{w})$.*

Proof. Let $\bar{\theta} \in \mathcal{A}$ be arbitrary. Then,

$$\begin{aligned} \frac{d}{dt} d_\psi(\bar{\theta} \parallel \hat{\theta}(t)) &= -\frac{1}{m} \sum_{i=1}^m \left(u(\langle \hat{\theta}(t), \alpha(\mathbf{x}_i) \rangle) - y_i \right) \langle \hat{\theta}(t) - \bar{\theta}, \alpha(\mathbf{x}_i) \rangle, \\ &= -\frac{1}{m} \sum_{i=1}^m \left(u(\langle \hat{\theta}(t), \alpha(\mathbf{x}_i) \rangle) - y_i \right) \left(\langle \hat{\theta}(t), \alpha(\mathbf{x}_i) \rangle - u^{-1}(y_i) \right). \end{aligned}$$

Above, we used that $\bar{\theta} \in \mathcal{A}$ and that $u(\cdot)$ is invertible, so that $u(\langle \bar{\theta}, \alpha(\mathbf{x}_i) \rangle) = y_i$ implies that $\langle \bar{\theta}, \alpha(\mathbf{x}_i) \rangle = u^{-1}(y_i)$. For clarity, define the error on example i as $\tilde{y}_i(\hat{\theta}(t)) = u(\langle \hat{\theta}(t), \alpha(\mathbf{x}_i) \rangle) - y_i$. Integrating both sides of the above from 0 to ∞ , we find that

$$d_\psi(\bar{\theta} \parallel \hat{\theta}_\infty) = d_\psi(\bar{\theta} \parallel \hat{\theta}(0)) - \frac{1}{m} \sum_{i=1}^m \int_0^\infty \left(\tilde{y}_i(\hat{\theta}(t)) \left(\langle \hat{\theta}(t), \alpha(\mathbf{x}_i) \rangle - u^{-1}(y_i) \right) \right) dt.$$

The above relation is true for any $\bar{\theta} \in \mathcal{A}$. Furthermore, the integral on the right-hand side is independent of $\bar{\theta}$. Hence the $\arg \min$ of the two Bregman divergences must be equal, which shows that $\hat{\theta}_\infty = \arg \min_{\bar{\theta} \in \mathcal{A}} d_\psi(\bar{\theta} \parallel \hat{\theta}(0))$. Choosing $\hat{\theta}(0) = \arg \min_{\mathbf{w} \in \mathbb{R}^d} \psi(\mathbf{w})$ completes the proof. \square

Theorem 3.2 elucidates the implicit bias of the Reflectron. Out of all possible interpolating parameters, the Reflectron finds those that minimize the Bregman divergence between the manifold of interpolating parameters and the initialization.

4 Vector-valued GLMs

In this section, we consider an extension to the case of vector-valued target variables $\mathbf{y}_i \in \mathbb{R}^n$. We assume that $\mathbf{u}(\mathbf{x})_i = u_i(x_i)$ where each u_i is L_i -Lipschitz and nondecreasing in its argument. We define the expected and empirical error measures in this setting by replacing squared terms with squared Euclidean norms in the definitions (1) and (2).

In many cases, it is desirable to allow for weight sharing between output variables in a model. For instance, if a vector-valued GLM estimation problem originates in a control or system identification context, parameters can have physical meaning and may appear in multiple equations. Similarly, convolutional neural networks exploit weight sharing as a beneficial prior for imposing translation equivariance. We can provably learn and implicitly regularize weight-shared GLMs via a vector-valued Reflectron. Define the dynamics

$$\frac{d}{dt} \nabla \psi(\hat{\theta}) = -\frac{1}{m} \sum_{i=1}^m \mathbf{A}^T(\mathbf{x}_i) \left(\mathbf{u}(\mathbf{A}(\mathbf{x}_i) \hat{\theta}) - \mathbf{y}_i \right) \quad (7)$$

with $\hat{\theta} \in \mathbb{R}^p$, $\mathbf{A}(\mathbf{x}_i) \in \mathbb{R}^{n \times p}$, and $\psi : \mathbb{R}^p \rightarrow \mathbb{R}^p$ convex. Note that (7) encompasses models of the form $\mathbf{h}(\mathbf{x}) = \mathbf{u}(\hat{\Theta}\alpha(\mathbf{x}))$ with $\hat{\Theta} \in \mathbb{R}^{n \times q}$ and $\alpha(\mathbf{x}) \in \mathbb{R}^q$ by unraveling $\hat{\Theta}$ into a vector of size nq and defining $\mathbf{A}(\mathbf{x})$ appropriately in terms of $\alpha(\mathbf{x})$. Appendix D discusses this case explicitly, where tighter bounds are attainable and matrix-valued regularizers can be used. Our work thus generalizes the model of Foster et al. (2020) to the case of shared parameters and mirror descent. It is similar in spirit to the Convotron of Goel et al. (2018), but exploits mirror descent and applies for vector-valued outputs. (7) could in principle be extended to provably learn regularized single-layer convolutional networks with multiple outputs via the distributional assumptions of Goel et al. (2018), which allow an application of average pooling.

We can state analogous guarantees as in the scalar-valued case. We begin with convergence.

Lemma 4.1 (Convergence of the vector-valued Reflectron for a realizable dataset). *Suppose that $\{\mathbf{x}_i, \mathbf{y}_i\}_{i=1}^m$ are drawn i.i.d. from a distribution \mathcal{D} supported on $\mathcal{X} \times [0, 1]^n$ and that Assumption 3.1 is satisfied where the component functions $\mathbf{u}(\mathbf{x})_i = u_i(x_i)$ are known, nondecreasing, and L_i -Lipschitz functions. Let ψ be any convex function with invertible Hessian over the trajectory $\hat{\theta}(t)$. Then $\hat{\varepsilon}(\mathbf{h}_t) \rightarrow 0$ where $\mathbf{h}_t(\mathbf{x}) = \mathbf{u}(\mathbf{A}(\mathbf{x})\hat{\theta})$ is the hypothesis with parameters output by the vector-valued Reflectron (7) at time t with $\hat{\theta}(0)$ arbitrary. Furthermore, $\inf_{t' \in [0, t]} \{\hat{\varepsilon}(\mathbf{h}_{t'})\} \leq \mathcal{O}(\frac{1}{t})$.*

The proof is given in Appendix A.1. As in the scalar-valued case, the choice of ψ implicitly biases $\hat{\theta}$.

Theorem 4.1 (Implicit regularization of the vector-valued Reflectron). *Consider the setting of Lemma 4.1. Assume that $\hat{\theta}(t) \rightarrow \hat{\theta}_\infty$ where $\hat{\theta}_\infty$ interpolates the data, and assume that $\mathbf{u}(\cdot)$ is invertible. Then $\hat{\theta}_\infty = \arg \min_{\bar{\theta} \in \mathcal{A}} d_\psi(\bar{\theta} \parallel \hat{\theta}(0))$ where \mathcal{A} is defined analogously as in Theorem 3.2. In particular, if $\hat{\theta}(0) = \arg \min_{\mathbf{w} \in \mathbb{R}^d} \psi(\mathbf{w})$, then $\hat{\theta}_\infty = \arg \min_{\bar{\theta} \in \mathcal{A}} \psi(\bar{\theta})$.*

The proof is given in Appendix A.2. Finally, we may also state a statistical guarantee for (7).

Theorem 4.2 (Statistical guarantees for the vector-valued Reflectron). *Suppose that $\{\mathbf{x}_i, \mathbf{y}_i\}_{i=1}^m$ are drawn i.i.d. from a distribution supported on $\mathcal{X} \times [0, 1]^n$ with $\mathbb{E}[\mathbf{y}|\mathbf{x}] = \mathbf{u}(\mathbf{A}(\mathbf{x})\theta)$ for a known function $\mathbf{u}(\mathbf{x})$ and an unknown vector of parameters $\theta \in \mathbb{R}^p$. Assume that $\mathbf{u}(\mathbf{x})_i = u_i(x_i)$ where each $u_i : \mathcal{X}_i \rightarrow [0, 1]$ is L_i -Lipschitz and nondecreasing in its argument. Assume that $\mathbf{A} : \mathcal{X} \rightarrow \mathbb{R}^{n \times p}$ is a known matrix with $\|\mathbf{A}(\mathbf{x})\|_2 \leq C$ for all $\mathbf{x} \in \mathcal{X}$. Further assume that $\|\alpha_i(\mathbf{x})\|_2 \leq C_r$ for $i = 1, \dots, n$ where $\alpha_i(\mathbf{x})$ is the i^{th} row of $\mathbf{A}(\mathbf{x})$. Let $d_\psi(\theta \parallel \mathbf{0}) \leq \frac{\sigma}{2} W^2$ where ψ is σ -strongly convex with respect to $\|\cdot\|_2$ and $W > 0$ is a constant. Then, for any $\delta \in (0, 1)$ with probability at least $1 - \delta$ over the draws of $\{\mathbf{x}_i, \mathbf{y}_i\}$, there exists some time $t < \mathcal{O}\left(\frac{\sigma W}{C\sqrt{n}} \sqrt{m/\log(1/\delta)}\right)$ such that the hypothesis $\mathbf{h}_t(\mathbf{x}) = \mathbf{u}(\mathbf{A}(\mathbf{x})\hat{\theta}(t))$ satisfies*

$$\begin{aligned}\hat{\varepsilon}(\mathbf{h}_t) &\leq \mathcal{O}\left(\frac{\max_k \{L_k\} CW}{\sqrt{m}} \sqrt{n \log(1/\delta)}\right), \\ \varepsilon(\mathbf{h}_t) &\leq \mathcal{O}\left(\frac{\max_k \{L_k\} W}{\sqrt{m}} \left(C_r n^{3/2} + C \sqrt{n \log(1/\delta)}\right)\right)\end{aligned}$$

where $\hat{\theta}(t)$ is output by the vector-valued Reflectron (7) at time t with $\hat{\theta}(0) = \mathbf{0}$.

The proof is given in Appendix A.3.

5 Simulations

As a simple illustration of our theoretical results, we perform classification on the MNIST dataset using a single-layer multiclass classification model. Details of the simulation setup can be found in Appendix B.1. In Figure 1A we show the empirical risk and generalization error trajectories for the Reflectron with $\psi(\cdot) = \|\cdot\|_{1,1}^2$ and $\psi(\cdot) = \|\cdot\|_2^2$. The latter option reduces to the GLM-tron while the first, following Theorem 3.2, approximates the l_1 norm and imposes sparsity. The dynamics are integrated with the `dop853` integrator from `scipy.integrate.ode`. Both choices converge to similar values of err and $\hat{\text{err}}$. In Figure 1B, we show the training and test set accuracy. Both choices

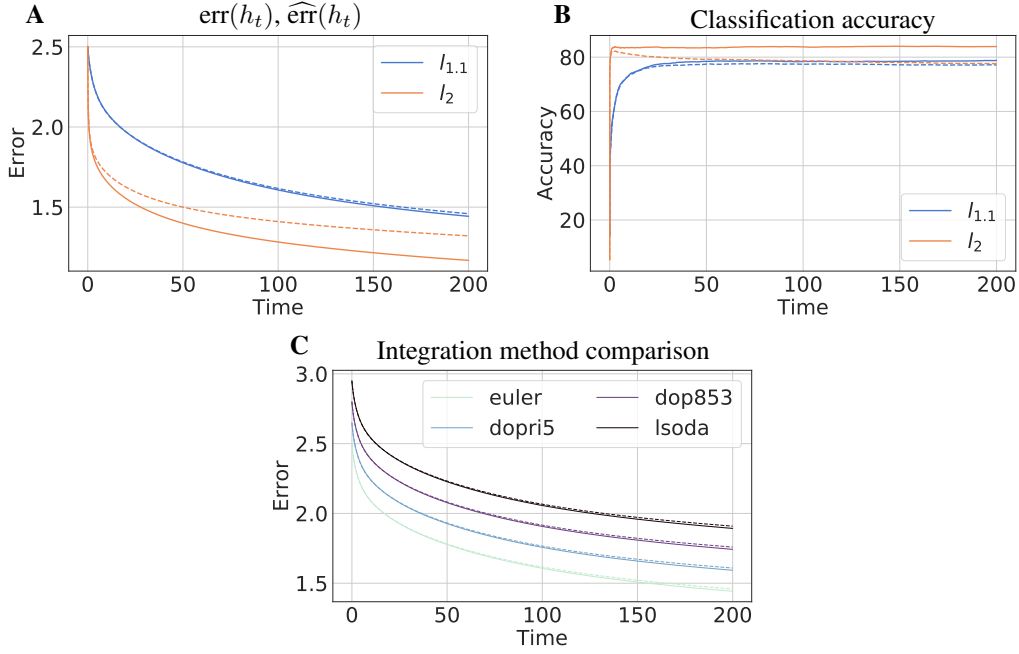


Figure 1: (A) Trajectories of the empirical risk $\widehat{\text{err}}(h_t)$ and generalization error $\text{err}(h_t)$. $\widehat{\text{err}}(h_t)$ is shown in solid while $\text{err}(h_t)$ is shown dashed. (B) Trajectories of the training and test set accuracy. Training is shown in solid while testing is shown dashed. (C) A comparison of the empirical risk and generalization error dynamics as a function of the integration method with $\psi(\cdot) = \|\cdot\|_{1.1}^2$. All solid curves and all dashed curves lie directly on top of each other and are shifted for visual clarity.

of norm converge to similar accuracy values. In Figure 1C, we show the curves $\widehat{\text{err}}(h_t)$ and $\text{err}(h_t)$ with $\psi(\cdot) = \|\cdot\|_{1.1}^2$ for four integration methods. The curves lie directly on top of each other and are shifted arbitrarily for clarity. This agreement highlights the validity of our continuous-time analysis, and that many possible discrete-time algorithms are captured by the continuous-time dynamics.

In Figure 2, we show histograms of the final parameter matrices learned by the Reflectron with $\psi(\cdot) = \|\cdot\|_{1.1}^2$ and $\psi(\cdot) = \|\cdot\|_2^2$. The histograms validate the prediction of Theorem 3.2. A sparse vector is found for $\psi(\cdot) = \|\cdot\|_{1.1}^2$, which obtains similar accuracy values to $\psi(\cdot) = \|\cdot\|_2^2$, as seen in Fig. 1C. 73.51% of parameters have magnitude less than 10^{-3} for $\psi(\cdot) = \|\cdot\|_{1.1}^2$, while only 12.27% do for $\psi(\cdot) = \|\cdot\|_2^2$. Future work will apply the Reflectron to models that combine a fixed expressive representation of the data with sparse learning, such as the scattering transform (Mallat, 2011; Bruna and Mallat, 2012; Talmon et al., 2015; Oyallon et al., 2019; Zarka et al., 2019).

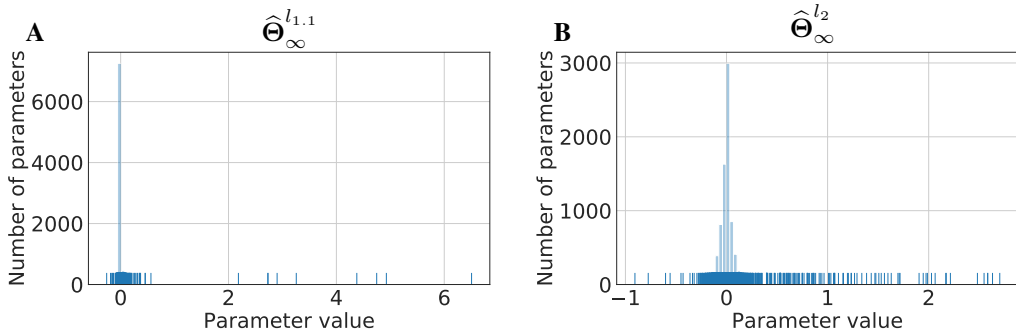


Figure 2: Histograms of parameter values for (A) the parameters found by the Reflectron with $\psi = \|\cdot\|_{1.1}^2$, and (B) the parameters found by the Reflectron with $\psi = \|\cdot\|_2^2$. This choice reduces to the GLM-tron. 73.51% of parameters have magnitude less than 10^{-3} with $\psi(\cdot) = \|\cdot\|_{1.1}^2$, while only 12.27% do for $\psi(\cdot) = \|\cdot\|_2^2$. Lowering this threshold shows that the $l_{1.1}$ regularized solution has many near-zero parameters, while the l_2 solution is diffuse.

6 Broader Impact

In this work, we developed mirror-descent like variants of the GLM-tron algorithm of Kakade et al. (2011). We proved guarantees on convergence and generalization, and characterized the implicit bias of our algorithms in terms of the potential function ψ . We generalized our results to the case of vector-valued target variables while allowing for the possibility of weight sharing between outputs. Our algorithms have applications in several settings. Using the techniques in Foster et al. (2020), they may be generalized to the adaptive control context for provably regularized online learning and control of stochastic dynamical systems. Applications in control will advance automation, but may have negative downstream consequences for those working in areas that can be replaced by adaptive control or robotic systems. Our algorithms can also be used for recovering the weights of a continuous- or discrete-time recurrent neural network from online data, which may have applications in recurrent network pruning (via sparsity promoting biases such as an l_1 approximation), or in computational neuroscience.

Acknowledgments and Disclosure of Funding

We thank Stephen Tu for many helpful discussions.

References

- Amari, S.-i. (1998). Natural gradient works efficiently in learning. *Neural Computation*, 10(2):251–276.
- Azizan, N. and Hassibi, B. (2019). Stochastic gradient/mirror descent: Minimax optimality and implicit regularization. In *International Conference on Learning Representations*.
- Azizan, N., Lale, S., and Hassibi, B. (2019). Stochastic mirror descent on overparameterized nonlinear models: Convergence, implicit regularization, and generalization. *arXiv:1906.03830*.
- Bai, S., Kolter, J. Z., and Koltun, V. (2019). Deep equilibrium models. *arXiv:1909.01377*.
- Bartlett, P. L., Long, P. M., Lugosi, G., and Tsigler, A. (2019). Benign overfitting in linear regression. *arXiv:1906.11300*.
- Bartlett, P. L. and Mendelson, S. (2002). Rademacher and gaussian complexities: Risk bounds and structural results. *J. Mach. Learn. Res.*, 3:463–482.
- Beck, A. and Teboulle, M. (2003). Mirror descent and nonlinear projected subgradient methods for convex optimization. *Operations Research Letters*, 31(3):167 – 175.
- Belkin, M., Hsu, D., Ma, S., and Mandal, S. (2019a). Reconciling modern machine-learning practice and the classical bias–variance trade-off. *Proceedings of the National Academy of Sciences*, 116(32):15849–15854.
- Belkin, M., Hsu, D., and Xu, J. (2019b). Two models of double descent for weak features. *arXiv:1903.07571*.
- Betancourt, M., Jordan, M. I., and Wilson, A. C. (2018). On symplectic optimization. *arXiv:1802.03653*.
- Boffi, N. M. and Slotine, J.-J. E. (2019). Higher-order algorithms and implicit regularization for nonlinearly parameterized adaptive control. *arXiv:1912.13154*.
- Boffi, N. M. and Slotine, J.-J. E. (2020). A continuous-time analysis of distributed stochastic gradient. *Neural Computation*, 32(1):36–96.
- Bregman, L. (1967). The relaxation method of finding the common point of convex sets and its application to the solution of problems in convex programming. *USSR Computational Mathematics and Mathematical Physics*, 7(3):200 – 217.
- Bruna, J. and Mallat, S. (2012). Invariant scattering convolution networks. *arXiv:1203.1513*.

- Butcher, J. (2001). *Numerical methods for ordinary differential equations in the 20th century*.
- Chen, R. T. Q., Rubanova, Y., Bettencourt, J., and Duvenaud, D. (2018). Neural ordinary differential equations. *arXiv:1806.07366*.
- Foster, D. J., Rakhlin, A., and Sarkar, T. (2020). Learning nonlinear dynamical systems from a single trajectory. *arXiv:2004.14681*.
- Goel, S. and Klivans, A. (2017). Learning neural networks with two nonlinear layers in polynomial time. *arXiv:1709.06010*.
- Goel, S., Klivans, A., and Meka, R. (2018). Learning one convolutional layer with overlapping patches. *arXiv:1802.02547*.
- Gunasekar, S., Lee, J., Soudry, D., and Srebro, N. (2018a). Characterizing implicit bias in terms of optimization geometry. *arXiv:1802.08246*.
- Gunasekar, S., Lee, J. D., Soudry, D., and Srebro, N. (2018b). Implicit bias of gradient descent on linear convolutional networks. In *Advances in Neural Information Processing Systems 31*, pages 9461–9471. Curran Associates, Inc.
- Gunasekar, S., Woodworth, B., Bhojanapalli, S., Neyshabur, B., and Srebro, N. (2017). Implicit regularization in matrix factorization. *arXiv:1705.09280*.
- Hastie, T., Montanari, A., Rosset, S., and Tibshirani, R. J. (2019). Surprises in high-dimensional ridgeless least squares interpolation. *arXiv:1903.08560*.
- Kakade, S., Kalai, A. T., Kanade, V., and Shamir, O. (2011). Efficient learning of generalized linear and single index models with isotonic regression. *arXiv:1104.2018*.
- Kakade, S. M., Sridharan, K., and Tewari, A. (2009). On the complexity of linear prediction: Risk bounds, margin bounds, and regularization. In Koller, D., Schuurmans, D., Bengio, Y., and Bottou, L., editors, *Advances in Neural Information Processing Systems 21*, pages 793–800. Curran Associates, Inc.
- Kalai, A. T. and Sastry, R. (2009). The isotron algorithm: High-dimensional isotonic regression. In *Proceedings of the 22nd Annual Conference on Learning Theory (COLT)*, 2009.
- Krichene, W., Bayen, A., and Bartlett, P. L. (2015). Accelerated mirror descent in continuous and discrete time. In *Advances in Neural Information Processing Systems 28*, pages 2845–2853. Curran Associates, Inc.
- Lee, J. D., Simchowitz, M., Jordan, M. I., and Recht, B. (2016). Gradient descent converges to minimizers. *arXiv:1602.04915*.
- Mallat, S. (2011). Group invariant scattering. *arXiv:1101.2286*.
- Maurer, A. (2016). A vector-contraction inequality for rademacher complexities. *arXiv:1605.00251*.
- McCullagh, P. and Nelder, J. (1989). *Generalized Linear Models, Second Edition*. CRC Press.
- Mei, S. and Montanari, A. (2019). The generalization error of random features regression: Precise asymptotics and double descent curve. *arXiv:1908.05355*.
- Muthukumar, V., Vodrahalli, K., and Sahai, A. (2019). Harmless interpolation of noisy data in regression. In *2019 IEEE International Symposium on Information Theory (ISIT)*, pages 2299–2303.
- Nacson, M. S., Lee, J. D., Gunasekar, S., Savarese, P. H. P., Srebro, N., and Soudry, D. (2018). Convergence of gradient descent on separable data. *arXiv:1803.01905*.
- Nesterov, Y. (1983). A Method for Solving a Convex Programming Problem with Convergence Rate $O(1/k^2)$. *Soviet Mathematics Doklady*, 26:367–372.
- Nock, R. and Menon, A. K. (2020). Supervised learning: No loss no cry. *arXiv:2002.03555*.

- Oyallon, E., Zagoruyko, S., Huang, G., Komodakis, N., Lacoste-Julien, S., Blaschko, M., and Belilovsky, E. (2019). Scattering networks for hybrid representation learning. *IEEE Transactions on Pattern Analysis and Machine Intelligence*, 41(9):2208–2221.
- Pascanu, R. and Bengio, Y. (2013). Revisiting natural gradient for deep networks. *arXiv:1301.3584*.
- Slotine, J.-J. and Li, W. (1991). *Applied Nonlinear Control*. Prentice Hall.
- Soudry, D., Hoffer, E., Nacson, M. S., Gunasekar, S., and Srebro, N. (2018). The implicit bias of gradient descent on separable data. *J. Mach. Learn. Res.*, 19(1):2822–2878.
- Su, W., Boyd, S., and Candès, E. J. (2016). A differential equation for modeling nesterov’s accelerated gradient method: Theory and insights. *Journal of Machine Learning Research*, 17(153):1–43.
- Sur, P. and Candès, E. J. (2019). A modern maximum-likelihood theory for high-dimensional logistic regression. *Proceedings of the National Academy of Sciences*, 116(29):14516–14525.
- Talmon, R., Mallat, S., Zaveri, H., and Coifman, R. R. (2015). Manifold learning for latent variable inference in dynamical systems. *IEEE Transactions on Signal Processing*, 63(15):3843–3856.
- Tyukin, I. Y., Prokhorov, D. V., and van Leeuwen, C. (2007). Adaptation and parameter estimation in systems with unstable target dynamics and nonlinear parametrization. *IEEE Transactions on Automatic Control*, 52(9):1543–1559.
- Wainwright, M. J. (2019). *High-Dimensional Statistics: A Non-Asymptotic Viewpoint*. Cambridge University Press.
- Wibisono, A., Wilson, A. C., and Jordan, M. I. (2016). A variational perspective on accelerated methods in optimization. *Proceedings of the National Academy of Sciences*, 113(47):E7351–E7358.
- Wilson, A. C., Recht, B., and Jordan, M. I. (2016). A lyapunov analysis of momentum methods in optimization. *arXiv:1611.02635*.
- Woodworth, B., Gunasekar, S., Lee, J. D., Moroshko, E., Savarese, P., Golan, I., Soudry, D., and Srebro, N. (2020). Kernel and rich regimes in overparametrized models. *arXiv:2002.09277*.
- Zarka, J., Thiry, L., Angles, T., and Mallat, S. (2019). Deep network classification by scattering and homotopy dictionary learning. *arXiv:1910.03561*.
- Zhang, C., Bengio, S., Hardt, M., Recht, B., and Vinyals, O. (2016). Understanding deep learning requires rethinking generalization. *arXiv:1611.03530*.
- Zhang, J., Mokhtari, A., Sra, S., and Jadbabaie, A. (2018). Direct runge-kutta discretization achieves acceleration. *arXiv:1805.00521*.

A Omitted proofs

A.1 Proof of Lemma 4.1

Proof. The proof is analogous to Lemma 3.1. We have that

$$\dot{\hat{\boldsymbol{\theta}}} = -\frac{1}{m} \sum_{i=1}^m \left(\nabla^2 \psi(\hat{\boldsymbol{\theta}}) \right)^{-1} \mathbf{A}^T(\mathbf{x}_i) \left(\mathbf{u} \left(\mathbf{A}(\mathbf{x}_i) \hat{\boldsymbol{\theta}} \right) - \mathbf{u} \left(\mathbf{A}(\mathbf{x}_i) \boldsymbol{\theta} \right) \right),$$

so that

$$\begin{aligned} \frac{d}{dt} d_\psi(\boldsymbol{\theta} \parallel \hat{\boldsymbol{\theta}}) &= (\hat{\boldsymbol{\theta}} - \boldsymbol{\theta})^T \left(-\frac{1}{m} \sum_{i=1}^m \mathbf{A}^T(\mathbf{x}_i) \left(\mathbf{u} \left(\mathbf{A}(\mathbf{x}_i) \hat{\boldsymbol{\theta}} \right) - \mathbf{u} \left(\mathbf{A}(\mathbf{x}_i) \boldsymbol{\theta} \right) \right) \right) \\ &= \sum_k (\hat{\theta}_k - \theta_k) \left(-\frac{1}{m} \sum_{i=1}^m \sum_j A_{jk}(\mathbf{x}_i) \left(u_j \left(\sum_k A_{jk}(\mathbf{x}_i) \hat{\theta}_k \right) - u_j \left(\sum_k A_{jk}(\mathbf{x}_i) \theta_k \right) \right) \right) \\ &= -\frac{1}{m} \sum_{i=1}^m \sum_j \left[\left(u_j \left(\sum_k A_{jk}(\mathbf{x}_i) \hat{\theta}_k \right) - u_j \left(\sum_k A_{jk}(\mathbf{x}_i) \theta_k \right) \right) \left(\sum_k A_{jk}(\mathbf{x}_i) (\hat{\theta}_k - \theta_k) \right) \right] \\ &\leq -\frac{1}{m} \sum_{i=1}^m \sum_j \frac{1}{L_j} \left(u_j \left(\sum_k A_{jk}(\mathbf{x}_i) \hat{\theta}_k \right) - u_j \left(\sum_k A_{jk}(\mathbf{x}_i) \theta_k \right) \right)^2 \\ &\leq -\frac{1}{m \max_k \{L_k\}} \sum_{i=1}^m \left\| \mathbf{u} \left(\mathbf{A}(\mathbf{x}_i) \hat{\boldsymbol{\theta}} \right) - \mathbf{u} \left(\mathbf{A}(\mathbf{x}_i) \boldsymbol{\theta} \right) \right\|^2 \\ &= -\frac{1}{\max_k \{L_k\}} \hat{\varepsilon}(\mathbf{h}_t) \leq 0 \end{aligned}$$

The conclusions of the lemma follow identically by the machinery of the proof of Lemma 3.1. \square

A.2 Proof of Theorem 4.1

Proof. The proof follows the same structure as in the scalar-valued case. Let $\bar{\boldsymbol{\theta}} \in \mathcal{A}$. Then,

$$\begin{aligned} \frac{d}{dt} d_\psi(\bar{\boldsymbol{\theta}} \parallel \hat{\boldsymbol{\theta}}) &= (\hat{\boldsymbol{\theta}} - \bar{\boldsymbol{\theta}})^T \left(-\frac{1}{m} \sum_{i=1}^m \mathbf{A}^T(\mathbf{x}_i) \left(\mathbf{u} \left(\mathbf{A}(\mathbf{x}_i) \hat{\boldsymbol{\theta}} \right) - \mathbf{y}_i \right) \right) \\ &= \text{Tr} \left[(\hat{\boldsymbol{\theta}} - \bar{\boldsymbol{\theta}})^T \left(-\frac{1}{m} \sum_{i=1}^m \mathbf{A}^T(\mathbf{x}_i) \left(\mathbf{u} \left(\mathbf{A}(\mathbf{x}_i) \hat{\boldsymbol{\theta}} \right) - \mathbf{y}_i \right) \right) \right] \\ &= -\frac{1}{m} \sum_{i=1}^m \text{Tr} \left[(\hat{\boldsymbol{\theta}} - \bar{\boldsymbol{\theta}})^T \mathbf{A}^T(\mathbf{x}_i) \left(\mathbf{u} \left(\mathbf{A}(\mathbf{x}_i) \hat{\boldsymbol{\theta}} \right) - \mathbf{y}_i \right) \right] \\ &= -\frac{1}{m} \sum_{i=1}^m \text{Tr} \left[\left(\mathbf{u} \left(\mathbf{A}(\mathbf{x}_i) \hat{\boldsymbol{\theta}} \right) - \mathbf{y}_i \right) (\hat{\boldsymbol{\theta}} - \bar{\boldsymbol{\theta}})^T \mathbf{A}^T(\mathbf{x}_i) \right] \\ &= -\frac{1}{m} \sum_{i=1}^m \left(\mathbf{u} \left(\mathbf{A}(\mathbf{x}_i) \hat{\boldsymbol{\theta}} \right) - \mathbf{y}_i \right)^T \mathbf{A}(\mathbf{x}_i) (\hat{\boldsymbol{\theta}} - \bar{\boldsymbol{\theta}}) \\ &= -\frac{1}{m} \sum_{i=1}^m \left(\mathbf{u} \left(\mathbf{A}(\mathbf{x}_i) \hat{\boldsymbol{\theta}} \right) - \mathbf{y}_i \right)^T \left(\mathbf{A}(\mathbf{x}_i) \hat{\boldsymbol{\theta}} - \mathbf{u}^{-1}(\mathbf{y}_i) \right) \end{aligned}$$

In the derivation above, we have replaced $\mathbf{A}(\mathbf{x}_i) \bar{\boldsymbol{\theta}}$ by $\mathbf{u}^{-1}(\mathbf{y}_i)$ following our assumptions that $\bar{\boldsymbol{\theta}} \in \mathcal{A}$ and \mathbf{u} is invertible. Integrating both sides of the above from 0 to ∞ , we find that

$$d_\psi(\bar{\boldsymbol{\theta}} \parallel \hat{\boldsymbol{\theta}}_\infty) = d_\psi(\bar{\boldsymbol{\theta}} \parallel \hat{\boldsymbol{\theta}}(0)) - \frac{1}{m} \sum_{i=1}^m \int_0^\infty \left(\mathbf{u} \left(\mathbf{A}(\mathbf{x}_i) \hat{\boldsymbol{\theta}}(t) \right) - \mathbf{y}_i \right)^T \left(\mathbf{A}(\mathbf{x}_i) \hat{\boldsymbol{\theta}}(t) - \mathbf{u}^{-1}(\mathbf{y}_i) \right) dt$$

The above relation is true for any $\bar{\boldsymbol{\theta}} \in \mathcal{A}$. Furthermore, the integral on the right-hand side is independent of $\bar{\boldsymbol{\theta}}$. Hence the arg min of the two Bregman divergences must be equal, which shows that

$$\hat{\boldsymbol{\theta}}_\infty = \arg \min_{\bar{\boldsymbol{\theta}} \in \mathcal{A}} d_\psi(\bar{\boldsymbol{\theta}} \parallel \hat{\boldsymbol{\theta}}(0))$$

Initializing $\hat{\boldsymbol{\theta}}(0) = \arg \min_{\mathbf{w} \in \mathbb{R}^p} \psi(\mathbf{w})$ completes the proof. \square

A.3 Proof of Theorem 4.2

Proof. Consider the rate of change of the Bregman divergence between the parameters for the Bayes-optimal predictor and the parameters produced by the Reflectron at time t . By the same method as in Lemma 4.1, we immediately have

$$\frac{d}{dt} d_\psi(\boldsymbol{\theta} \parallel \hat{\boldsymbol{\theta}}) \leq -\frac{1}{\max_k \{L_k\}} \hat{\varepsilon}(\mathbf{h}_t) + \frac{1}{m} \sum_{i=1}^m (\mathbf{y}_i - \mathbf{u}(\mathbf{A}(\mathbf{x}_i)\boldsymbol{\theta}))^T \mathbf{A}(\mathbf{x}_i) (\hat{\boldsymbol{\theta}} - \boldsymbol{\theta})$$

Now, note that each $\frac{1}{C\sqrt{n}} (\mathbf{y}_i - \mathbf{u}(\mathbf{A}(\mathbf{x}_i)\boldsymbol{\theta}))^T \mathbf{A}(\mathbf{x}_i)$ is a zero-mean i.i.d. random variable with Euclidean norm bounded by 1 almost surely. Then, by Lemma C.1, $\|\frac{1}{C\sqrt{nm}} \sum_{i=1}^m (\mathbf{y}_i - \mathbf{u}(\mathbf{A}(\mathbf{x}_i)\boldsymbol{\theta}))^T \mathbf{A}(\mathbf{x}_i)\|_2 \leq \eta$ with probability at least $1 - \delta$ where $\eta = \frac{2(1+\sqrt{\log(1/\delta)/2})}{\sqrt{m}}$. Assuming that $\|\hat{\boldsymbol{\theta}}(t) - \boldsymbol{\theta}\|_2 \leq W$ at time t , we conclude that

$$\frac{d}{dt} d_\psi(\boldsymbol{\theta} \parallel \hat{\boldsymbol{\theta}}) \leq -\frac{1}{\max_k \{L_k\}} \hat{\varepsilon}(\mathbf{h}_t) + \sqrt{n}CW\eta.$$

Hence, either $\frac{d}{dt} d_\psi(\boldsymbol{\theta} \parallel \hat{\boldsymbol{\theta}}) < -\sqrt{n}CW\eta$, or $\hat{\varepsilon}(\mathbf{h}_t) \leq 2(\max_k \{L_k\})\sqrt{n}CW\eta$. In the latter case, our result is proven. In the former, by our assumptions $d_\psi(\boldsymbol{\theta} \parallel \mathbf{0}) = d_\psi(\boldsymbol{\theta} \parallel \hat{\boldsymbol{\theta}}(0)) \leq \frac{\sigma}{2}W^2$, and hence $\|\hat{\boldsymbol{\theta}}(0) - \boldsymbol{\theta}\| \leq W$ by σ -strong convexity of ψ with respect to $\|\cdot\|_2$. Furthermore, $\|\hat{\boldsymbol{\theta}}(t) - \boldsymbol{\theta}\| \leq \sqrt{\frac{2}{\sigma}} d_\psi(\boldsymbol{\theta} \parallel \hat{\boldsymbol{\theta}}(t)) \leq \sqrt{\frac{2}{\sigma}} d_\psi(\boldsymbol{\theta} \parallel \hat{\boldsymbol{\theta}}(0)) \leq W$. Thus it can be until at most

$$t_f = \frac{d_\psi(\boldsymbol{\theta} \parallel \hat{\boldsymbol{\theta}}(0))}{\sqrt{n}CW\eta} = \frac{\sigma/2W^2}{\sqrt{n}CW\eta} = \frac{\sigma W}{2\sqrt{n}C\eta}$$

until $\hat{\varepsilon}(\mathbf{h}_t) \leq 2\max_k \{L_k\}\sqrt{n}CW\eta$. Hence there is some \mathbf{h}_t with $t < t_f$ such that

$$\hat{\varepsilon}(\mathbf{h}_t) \leq \mathcal{O}\left(\sqrt{n}\max_k \{L_k\}CW\sqrt{\frac{\log(1/\delta)}{m}}\right).$$

Combining Theorems C.1 and C.2, we obtain a bound on the Rademacher complexity of the function class for each component of $\mathbf{u}(\mathbf{A}(\mathbf{x})\hat{\boldsymbol{\theta}})$,

$$\mathcal{R}_m(\mathcal{F}_k) \leq \mathcal{O}\left(\frac{L_k C_r W}{\sqrt{m}}\right).$$

Application of Theorem C.5 to bound the generalization error, noting that the square loss is \sqrt{n} -Lipschitz and \sqrt{n} -bounded over $[0, 1]^n$, gives us the bound

$$|\hat{\varepsilon}(\mathbf{h}_t) - \varepsilon(\mathbf{h}_t)| \leq \mathcal{O}\left(\frac{\max_k \{L_k\} C_r W n^{3/2}}{\sqrt{m}}\right) + \mathcal{O}\left(\sqrt{\frac{n \log(1/\delta)}{m}}\right)$$

which completes the proof. \square

B Further simulation details and results

B.1 MNIST simulation details

We implement the vector-valued Reflectron without weight sharing. Rather than implement the continuous-time dynamics (7), we directly utilize the dynamics (9), as they are more efficient without weight sharing. In Section 5, we show results for the mirror descent-like dynamics. Appendix B.2 shows similar results for the natural gradient-like dynamics. Our hypothesis at time t is given by

$$\mathbf{h}_t(\mathbf{x}) = \mathbf{u}\left(\widehat{\Theta}(t)\mathbf{x}\right)$$

where $\mathbf{u}(\cdot)$ is an elementwise sigmoid, $\mathbf{x} \in \mathbb{R}^{784}$ is an image from the MNIST dataset, and $\widehat{\Theta} \in \mathbb{R}^{10 \times 784}$ is a matrix of parameters to be learned. We use one-hot encoding on the class labels, and the predicted class is obtained by taking an $\arg \max$ over the components of $\mathbf{h}_t(\mathbf{x})$. A training set of size 5000 and a test set of size 10000 are both randomly selected from the overall dataset, so that the number of parameters $np > m$. The training data is pre-processed to have zero mean and unit variance. The testing data is shifted by the mean of the training data and normalized by the standard deviation of the training data. A value of $\Delta t = 0.05$ is used for all cases, up to adaptive timestepping performed by the black-box ODE solvers. Convergence speed can be different for different choices of ψ . To ensure convergence over similar timescales, we use a learning rate of $1/(1 - q)$ in the continuous-time dynamics with $\psi = \|\cdot\|_q^2$.

Because we use an elementwise sigmoid, the output of our model is not required to be a probability distribution over classes. This is equivalent to relaxing the requirement that the output classes be exclusive. However, the Reflectron works directly on the square loss rather than the negative log-likelihood, so it is not necessary for our model to output a probability distribution.

The square loss is not typically used in multiclass classification. Designing similar provable algorithms for other loss functions – such as the negative log-likelihood – and relaxing the elementwise Lipschitz condition – for applications to activations such as the softmax – is an interesting direction for future work. Similarly, tailoring the choice of ψ to the loss function, e.g. by using the self entropy, may lead to new algorithms with strong guarantees for specific application domains.

B.2 Natural gradient

In this section, we show that the same qualitative phenomena as displayed in Section 5 are observed when discretizing the natural gradient-like dynamics

$$\dot{\widehat{\Theta}} = -\frac{1}{m} \sum_{i=1}^m \left(\nabla^2 \psi(\widehat{\Theta}) \right)^{-1} \left(\mathbf{u}\left(\widehat{\Theta} \alpha(\mathbf{x}_i)\right) - \mathbf{y}_i \right) \alpha^T(\mathbf{x}_i). \quad (8)$$

Formally, (8) is equivalent to (7) without weight sharing (handled explicitly in Appendix D) in continuous-time, but will differ in an implementation due to discretization errors. We utilize the same simulation setup as described in Appendix B.1. Results are shown in Figure 3, where we display convergence of the empirical and expected risk in (A), convergence of the classification accuracy in (B), a histogram of the sparse solution found by choosing $\psi(\cdot) = \|\cdot\|_{1,1}^{1.1}$ in (C), and a comparison of integration methods in (D). $\psi(\cdot)$ is chosen as $\|\cdot\|_{1,1}^{1.1}$ rather than $\|\cdot\|_{1,1}^2$ as the former admits a diagonal Hessian, while the Hessian for the latter is dense. Conversely, the latter admits a simple inversion formula for the gradient, while the former does not. As predicted by Theorem 4.1, the natural gradient system implicitly regularizes the learned model, as indicated by the sparse matrix displayed in Figure 3C. While implicit regularization is only approximate for natural gradient systems in discrete-time for linear models (Gunasekar et al., 2018a), higher-order integration can ensure that the discrepancy between the natural gradient and mirror descent dynamics is small. This allows the choice of whichever method is computationally more efficient for the application – inverting the Hessian $\nabla^2 \psi(\cdot)$ or inverting the gradient $\nabla \psi(\cdot)$. Nevertheless, that implicit regularization is only approximate for this system can be seen by noting that 54.11% of parameters have magnitude less than 10^{-3} here, compared with 73.51% for the mirror descent-like dynamics.

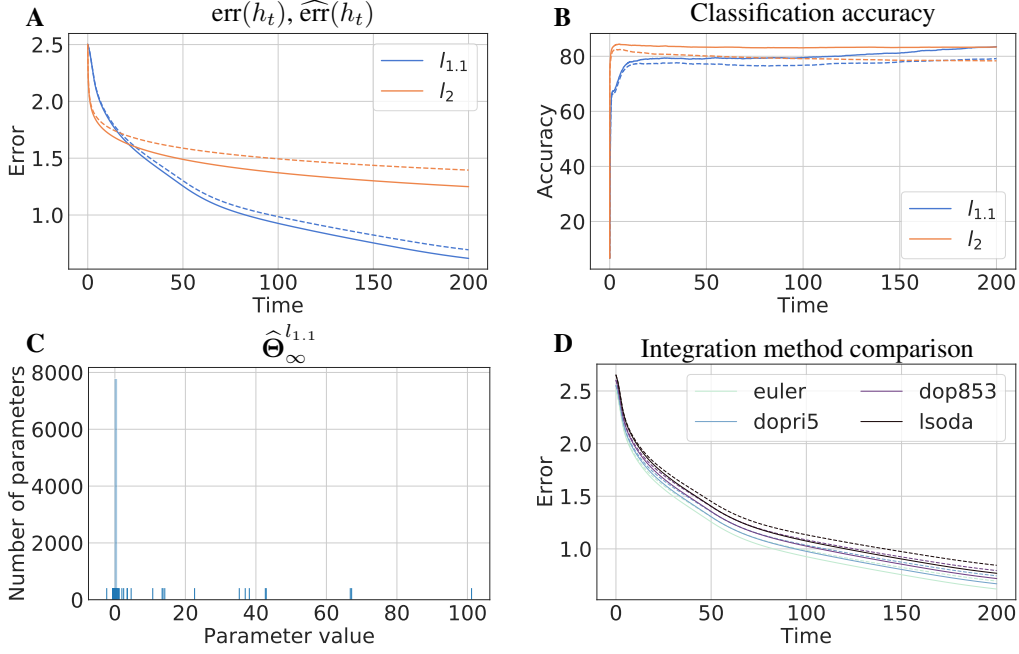


Figure 3: (A) Trajectories of the empirical risk $\widehat{\text{err}}(h_t)$ and generalization error $\text{err}(h_t)$ for the natural gradient-like dynamics (8). $\widehat{\text{err}}(h_t)$ is shown in solid while $\text{err}(h_t)$ is shown dashed. Comparison of the sparsity-promoting Reflectron with $\psi = \|\cdot\|_{1.1}^2$ to the GLM-Tron. (B) Classification accuracy over time. Training curve is shown in solid while the testing curve is shown dashed. (C) Histogram of parameters found by the $l_{1.1}$ -regularized Reflectron via natural gradient. The resulting parameter vector has 54.11% of entries with absolute value below 10^{-3} . (D) A comparison of integration methods of the dynamics. All solid curves and all dashed curves lie directly on top of each other and are shifted for clarity.

B.3 Synthetic dataset

Training examples $\{\mathbf{x}_i, y_i\}_{i=1}^m$ are generated according to the model

$$y_i = \sigma(\boldsymbol{\theta}^T \boldsymbol{\alpha}(\mathbf{x}_i)) + \xi_i$$

where $\sigma(\cdot)$ is the sigmoid function and $\xi_i \sim \text{Unif}(a_\xi, b_\xi)$ is a uniform noise term with $a_\xi = -b_\xi = .05$. The y_i values are clamped to lie in the interval $[0, 1]$ in the case that ξ_i pushes them over the boundary. $\boldsymbol{\alpha}(\mathbf{x}_i)$ is taken to be $\boldsymbol{\alpha}(\mathbf{x}_i) = \cos(\mathbf{V}\mathbf{x}_i)$ with $\mathbf{V} \in \mathbb{R}^{p \times k}$ a random matrix $V_{ij} \sim \mathcal{N}(0, 1)$. Each $\mathbf{x}_i \in \mathbb{R}^k$ is drawn i.i.d. from a Gaussian $\mathbf{x}_i \sim \mathcal{N}(0, \sigma_x^2)$ with $\sigma_x = 2$. Each component of $\boldsymbol{\theta}$ is also generated i.i.d. from a standard normal distribution $\theta_i \sim \mathcal{N}(0, 1)$. These values were chosen so as to not saturate the sigmoid and to get a range of $y_i \in [0, 1]$. We take $m = 100$, $k = 25$, and $p = 75$, so that $k < p < m$ but $\frac{p}{m} = \frac{3}{4}$, representing the modern regime of high-dimensional logistic regression where the classical assumption of $p \ll m$ is violated (Sur and Candès, 2019). We similarly generate a test set with 400 examples for estimation of $\text{err}(h_t)$. As an example of regression, we assume access to the real-valued y_i during model training rather than binary labels. A value of $\Delta t = 0.05$ is used for all cases, up to adaptive timestepping performed by the black-box ODE solvers. As in Appendix B.1, we rescale the learning rate to plot on similar timescales.

In Figure 4A, we show the empirical risk and generalization error trajectories for the Reflectron with $\psi(\cdot) = \|\cdot\|_{1.1}^2$ and $\psi(\cdot) = \|\cdot\|_2^2$. The dynamics are integrated with the lsoda integrator from `scipy.integrate.ode`. Both choices converge to similar values of err and $\widehat{\text{err}}$. In Figure 4B, we show the curves $\widehat{\text{err}}(h_t)$ and $\text{err}(h_t)$ with $\psi(\cdot) = \|\cdot\|_{1.1}^2$ for four integration methods. The curves lie directly on top of each other and are shifted arbitrarily for clarity.

In Figure 5, we show histograms of the parameter values for the Bayes-optimal predictor $\boldsymbol{\theta}$, as well as the final parameter values found by the Reflectron with $\psi(\cdot) = \|\cdot\|_{1.1}^2$ and $\psi(\cdot) = \|\cdot\|_2^2$. The histograms validate the prediction of Theorem 3.2. A sparse vector is found for $\psi = \|\cdot\|_{1.1}^2$, which obtains similar values of $\text{err}(h_t)$ to $\|\cdot\|_2^2$, as seen in Fig. 4A.

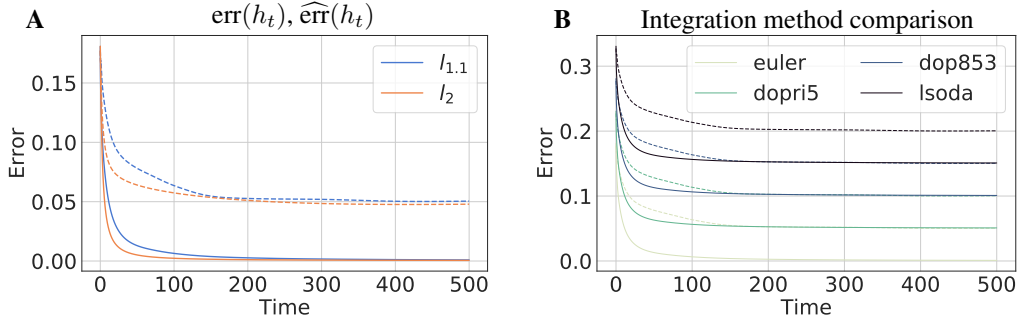


Figure 4: Trajectories of the empirical risk $\widehat{\text{err}}(h_t)$ and generalization error $\text{err}(h_t)$. $\widehat{\text{err}}(h_t)$ is shown in solid while $\text{err}(h_t)$ is shown dashed. (A) Comparison of the sparsity-promoting Reflectron with $\psi = \|\cdot\|_{1.1}^2$ to the GLM-Tron. (B) A comparison of the empirical risk and generalization error dynamics as a function of the integration method with $\psi(\cdot) = \|\cdot\|_{1.1}^2$. All solid curves and all dashed curves lie directly on top of each other and are shifted for clarity.

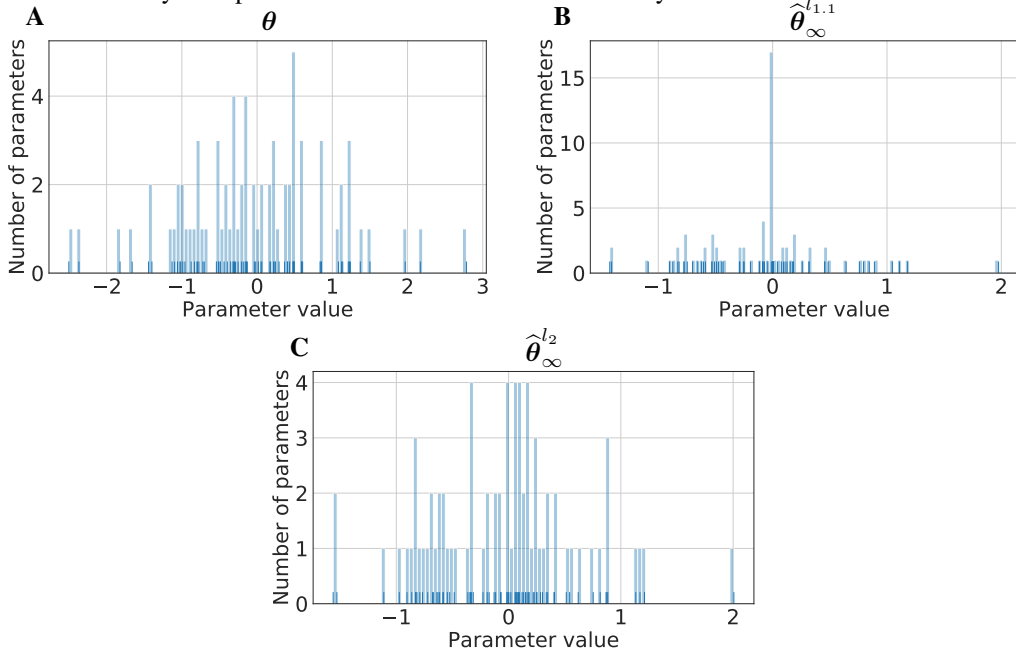


Figure 5: Histograms of parameter values for (A) the Bayes-optimal predictor θ , (B) the parameters found by the Reflectron with $\psi = \|\cdot\|_{1.1}^2$, and (C) the parameters found by the Reflectron with $\psi = \|\cdot\|_2^2$. This choice reduces to the GLM-Tron.

A similar discussion applies here as in Appendix B.1. The Reflectron is designed for minimizing the square loss, which is not typically used in logistic regression. Designing similar provable algorithms for other loss functions – such as the negative log-likelihood – and tailoring the choice of ψ to the loss function is an interesting opportunity for future research.

C Required results

In this section, we present some results required for our analysis. The following lemma is well-known, and may be readily obtained via application of a Hoeffding bound.

Lemma C.1. *Suppose $\mathbf{z}_1, \dots, \mathbf{z}_m$ are i.i.d. 0-mean random variables in a Hilbert space such that $\Pr(\|\mathbf{z}_i\| \leq 1) = 1$. Then, with probability at least $1 - \delta$,*

$$\left\| \frac{1}{m} \sum_{i=1}^m \mathbf{z}_i \right\| \leq 2 \left(\frac{1 + \sqrt{\log(1/\delta)/2}}{\sqrt{m}} \right)$$

The following theorem gives a bound on the Rademacher complexity of a linear predictor.

Theorem C.1 (Kakade et al. (2009)). *Let \mathcal{X} be a subset of a Hilbert space equipped with an inner product $\langle \cdot, \cdot \rangle$ such that for each $\mathbf{x} \in \mathcal{X}$, $\langle \mathbf{x}, \mathbf{x} \rangle \leq X^2$. Let $\mathcal{W} = \{\mathbf{x} \mapsto \langle \mathbf{x}, \mathbf{w} \rangle : \langle \mathbf{w}, \mathbf{w} \rangle \leq W^2\}$ be a class of linear functions. Then*

$$\mathcal{R}_m(\mathcal{W}) \leq XW \sqrt{\frac{1}{m}}$$

where $\mathcal{R}_m(\mathcal{W})$ is the Rademacher complexity of the function class \mathcal{W} ,

$$\mathcal{R}_m(\mathcal{W}) = \mathbb{E}_{\mathbf{x}_i, \epsilon_i} \left[\sup_{\mathbf{f} \in \mathcal{W}} \frac{1}{m} \sum_{i=1}^m \epsilon_i \mathbf{f}(\mathbf{x}_i) \right]$$

with ϵ_i Rademacher distributed random variables.

The following theorem is useful for bounding the Rademacher complexity of the generalized linear models considered in this work. It may also be used to bound the generalization error in terms of the Rademacher complexity of a function class.

Theorem C.2 (Bartlett and Mendelson (2002)). *Let $\phi : \mathbb{R} \rightarrow \mathbb{R}$ be L_ϕ -Lipschitz and suppose that $\phi(0) = 0$. Let \mathcal{F} be a class of functions. Then $\mathcal{R}_m(\phi \circ \mathcal{F}) \leq 2L_\phi \mathcal{R}_m(\mathcal{F})$.*

The following theorem allows for a bound on the generalization error if bounds on the empirical risk and the Rademacher complexity of the function class are known.

Theorem C.3 (Generalization error via Rademacher complexity (Bartlett and Mendelson, 2002)). *Let $\{\mathbf{x}_i, y_i\}_{i=1}^m$ be an i.i.d. sample from a distribution P over $\mathcal{X} \times \mathcal{Y}$ and let $\mathcal{L} : \mathcal{Y}' \times \mathcal{Y} \rightarrow \mathbb{R}$ be an L -Lipschitz and b -bounded loss function in its first argument. Let $\mathcal{F} = \{f \mid f : \mathcal{X} \rightarrow \mathcal{Y}'\}$ be a class of functions. For any positive integer $m \geq 0$ and any scalar $\delta \geq 0$,*

$$\sup_{f \in \mathcal{F}} \left| \frac{1}{m} \sum_{i=1}^m \mathcal{L}(f(\mathbf{x}_i), y_i) - \mathbb{E}_{(\mathbf{x}, y) \sim P} [\mathcal{L}(f(\mathbf{x}), y)] \right| \leq 4L\mathcal{R}_m(\mathcal{F}) + 2b \sqrt{\frac{2}{m} \log \left(\frac{1}{\delta} \right)}$$

with probability at least $1 - \delta$ over the draws of the $\{\mathbf{x}_i, y_i\}$.

The following theorem comes from the main result and the example in Section 4.2 of Maurer (2016). It enables us to bound the Rademacher complexity of the square loss composed with the link function \mathbf{u} in the vector-valued output case handled in Appendix D.

Theorem C.4 (Vector contraction inequality (Maurer, 2016)). *Let \mathcal{X} be a subset of a Hilbert space equipped with an inner product $\langle \cdot, \cdot \rangle$ such that for each $\mathbf{x} \in \mathcal{X}$, $\langle \mathbf{x}, \mathbf{x} \rangle \leq X^2$. Let $\mathcal{B}(\mathcal{X}, \mathbb{R}^n)$ be the set of bounded linear transformations from \mathcal{X} into \mathbb{R}^n . Define a class of functions $\mathcal{F} = \{\mathbf{x} \mapsto \mathbf{W}\mathbf{x} \mid \mathbf{W} \in \mathcal{B}(\mathcal{X}, \mathbb{R}^n), \|\mathbf{W}\| \leq W\}$. Let $h_i : \mathbb{R}^n \rightarrow \mathbb{R}$ have Lipschitz constant L . Then*

$$\mathbb{E}_{\epsilon_i} \left[\sup_{\mathbf{f} \in \mathcal{F}} \frac{1}{m} \sum_{i=1}^m \epsilon_i h_i(\mathbf{f}(\mathbf{x}_i)) \right] \leq \mathcal{O} \left(LXW \sqrt{\frac{n}{m}} \right).$$

where the ϵ_i are Rademacher random variables.

The following theorem is similar to Theorem C.4, but gives a weaker bound linear in the output dimension. See the main theorem and Section 4.1 in (Maurer, 2016).

Theorem C.5 (Weak vector contraction inequality (Maurer, 2016)). *Let \mathcal{X} be any set, let \mathcal{F} be a class of functions $f : \mathcal{X} \rightarrow \mathbb{R}^n$, and let $h_i : \mathbb{R}^n \rightarrow \mathbb{R}$ have Lipschitz constant L . Define $\mathcal{F}_k = \{\mathbf{x} \mapsto f_k(\mathbf{x}) : \mathbf{f}(\mathbf{x}) = (f_1(\mathbf{x}), f_2(\mathbf{x}), \dots, f_n(\mathbf{x})) \in \mathcal{F}\}$ as the projection onto the k^{th} coordinate class of \mathcal{F} . Then*

$$\mathbb{E}_{\epsilon_i} \left[\sup_{\mathbf{f} \in \mathcal{F}} \frac{1}{m} \sum_{i=1}^m \epsilon_i h_i(\mathbf{f}(\mathbf{x}_i)) \right] \leq \sqrt{2}L \sum_{k=1}^n \mathbb{E}_{\epsilon_i} \left[\sup_{f \in \mathcal{F}_k} \frac{1}{m} \sum_{i=1}^m \epsilon_i f(x_i) \right].$$

The following lemma is a technical result from functional analysis which has seen widespread application in adaptive control theory (Slotine and Li, 1991).

Lemma C.2 (Barbalat's Lemma). *Assume that $\lim_{t \rightarrow \infty} \int_0^t |x(\tau)| d\tau < \infty$. If $x(t)$ is uniformly continuous, then $\lim_{t \rightarrow \infty} x(t) = 0$.*

Note that a sufficient condition for uniform continuity of $x(t)$ is that $\dot{x}(t)$ is bounded.

D Vector-valued Reflectron without weight sharing

In this section, we handle the vector-valued Reflectron without weight sharing. We define the vector-valued Reflectron without weight sharing via the continuous-time dynamics

$$\frac{d}{dt} \nabla \psi \left(\hat{\Theta}(t) \right) = -\frac{1}{m} \sum_{i=1}^m \left(\mathbf{u} \left(\hat{\Theta} \alpha(\mathbf{x}_i) \right) - \mathbf{y}_i \right) \alpha^T(\mathbf{x}_i) \quad (9)$$

where $\psi : \mathbb{R}^{n \times p} \rightarrow \mathbb{R}$ is a strictly convex function on matrices. (9) is similar to running the scalar-valued Reflectron (5) on each component individually. However, analyzing it in the form (9) enables more general results on implicit regularization – which apply to the matrix $\hat{\Theta}$ directly rather than its rows – and tighter bounds on the generalization error.

We begin with a convergence theorem.

Lemma D.1 (Convergence of the vector-valued Reflectron without weight sharing for a realizable dataset). *Suppose that $\{\mathbf{x}_i, \mathbf{y}_i\}_{i=1}^m$ are drawn i.i.d. from a distribution \mathcal{D} supported on $\mathcal{X} \times [0, 1]^n$ and that Assumption 3.1 is satisfied where the component functions $\mathbf{u}(\mathbf{x})_i = u_i(x_i)$ are known, nondecreasing, and L_i -Lipschitz functions. Let ψ be any convex function with invertible Hessian tensor over the trajectory $\hat{\Theta}(t)$. Then $\hat{\varepsilon}(\mathbf{h}_t) \rightarrow 0$ where $\mathbf{h}_t(\mathbf{x}) = \mathbf{u} \left(\hat{\Theta}(t) \alpha(\mathbf{x}) \right)$ is the hypothesis with parameters output by the vector-valued Reflectron at time t with $\hat{\Theta}(0)$ arbitrary. Furthermore, $\inf_{t' \in [0, t]} \{\hat{\varepsilon}(\mathbf{h}_{t'})\} \leq \mathcal{O} \left(\frac{1}{t} \right)$.*

Proof. The proof is analogous to Lemma 3.1, but requires more technical manipulation of indices. Define the Bregman divergence in a natural way

$$d_\psi \left(\Theta \parallel \hat{\Theta} \right) = \psi(\Theta) - \psi(\hat{\Theta}) - \sum_{ij} \frac{\partial \psi(\hat{\Theta})}{\partial \hat{\Theta}_{ij}} (\Theta_{ij} - \hat{\Theta}_{ij}).$$

Then we have the equality

$$\frac{d}{dt} d_\psi \left(\Theta \parallel \hat{\Theta} \right) = \left(\hat{\Theta} - \Theta \right) : \nabla^2 \psi \left(\hat{\Theta} \right) : \dot{\hat{\Theta}}$$

where for a symmetric four-tensor \mathbf{A} , the real number $\mathbf{C} : \mathbf{A} : \mathbf{B} = \sum_{ijkl} C_{ij} A_{ijkl} B_{kl}$ and $\nabla^2 \psi(\hat{\Theta})_{ijkl} = \frac{\partial^2 \psi(\hat{\Theta})}{\partial \hat{\Theta}_{kl} \partial \hat{\Theta}_{ij}}$. Note that the inverse Hessian tensor is a map $(\nabla^2 \psi(\cdot))^{-1} : \mathbb{R}^{n \times p} \rightarrow \mathbb{R}^{n \times p}$. By definition, (9) then implies that

$$\dot{\hat{\Theta}} = -\frac{1}{m} \sum_{i=1}^m \left(\nabla^2 \psi \left(\hat{\Theta} \right) \right)^{-1} \left(\mathbf{u} \left(\hat{\Theta} \alpha(\mathbf{x}_i) \right) - \mathbf{u} \left(\Theta \alpha(\mathbf{x}_i) \right) \right) \alpha^T(\mathbf{x}_i),$$

so that

$$\begin{aligned}
\frac{d}{dt}d_\psi(\Theta \parallel \hat{\Theta}) &= (\hat{\Theta} - \Theta) : \left(-\frac{1}{m} \sum_{i=1}^m \left(\mathbf{u}(\hat{\Theta}\alpha(\mathbf{x}_i)) - \mathbf{u}(\Theta\alpha(\mathbf{x}_i)) \right) \alpha^T(\mathbf{x}_i) \right) \\
&= \sum_{kl} (\hat{\Theta} - \Theta)_{kl} \left(-\frac{1}{m} \sum_{i=1}^m \left(\mathbf{u}(\hat{\Theta}\alpha(\mathbf{x}_i)) - \mathbf{u}(\Theta\alpha(\mathbf{x}_i)) \right) \alpha^T(\mathbf{x}_i) \right)_{kl} \\
&= \sum_{kl} (\hat{\Theta}_{kl} - \Theta_{kl}) \left(-\frac{1}{m} \sum_{i=1}^m \left(u_k \left(\sum_q \hat{\Theta}_{kq} \alpha_q(\mathbf{x}_i) \right) - u_k \left(\sum_q \Theta_{kq} \alpha_q(\mathbf{x}_i) \right) \right) \alpha_l(\mathbf{x}_i) \right) \\
&= -\frac{1}{m} \sum_i \left(\sum_{kl} (\hat{\Theta}_{kl} - \Theta_{kl}) \left(u_k \left(\sum_q \hat{\Theta}_{kq} \alpha_q(\mathbf{x}_i) \right) - u_k \left(\sum_q \Theta_{kq} \alpha_q(\mathbf{x}_i) \right) \right) \alpha_l(\mathbf{x}_i) \right) \\
&= -\frac{1}{m} \sum_i \left(\sum_k \left(u_k \left(\sum_q \hat{\Theta}_{kq} \alpha_q(\mathbf{x}_i) \right) - u_k \left(\sum_q \Theta_{kq} \alpha_q(\mathbf{x}_i) \right) \right) \left(\sum_q (\hat{\Theta}_{kq} - \Theta_{kq}) \alpha_q(\mathbf{x}_i) \right) \right) \\
&\leq -\frac{1}{m} \sum_i \sum_k \frac{1}{L_k} \left(u_k \left(\sum_q \hat{\Theta}_{kq} \alpha_q(\mathbf{x}_i) \right) - u_k \left(\sum_q \Theta_{kq} \alpha_q(\mathbf{x}_i) \right) \right)^2 \\
&= -\frac{1}{m \max_k \{L_k\}} \sum_i \left\| \mathbf{u}(\hat{\Theta}\alpha(\mathbf{x}_i)) - \mathbf{u}(\Theta\alpha(\mathbf{x}_i)) \right\|_2^2 \\
&= -\frac{1}{\max_k \{L_k\}} \hat{\varepsilon}(\mathbf{h}_t) \leq 0.
\end{aligned}$$

The conclusions of the Lemma follow identically by the machinery of the proof of Lemma 3.1. \square

In a similar manner, we can state a result on the implicit regularization of the matrix $\hat{\Theta}$.

Theorem D.1 (Implicit regularization of the vector-valued Reflectron without weight sharing). *Consider the setting of Lemma D.1. Assume that $\hat{\Theta}(t) \rightarrow \hat{\Theta}_\infty$ where $\hat{\Theta}_\infty$ interpolates the data, and assume that $\mathbf{u}(\cdot)$ is invertible. Then*

$$\hat{\Theta}_\infty = \arg \min_{\bar{\Theta} \in \mathcal{A}} d_\psi(\bar{\Theta} \parallel \hat{\Theta}(0))$$

where \mathcal{A} is defined analogously as in the proof of Theorem 3.2. In particular, if $\hat{\Theta}(0) = \arg \min_{\mathbf{W} \in \mathbb{R}^d} \psi(\mathbf{W})$, then $\hat{\Theta}_\infty = \arg \min_{\bar{\Theta} \in \mathcal{A}} \psi(\bar{\Theta})$.

Proof. The proof follows the same structure as in the scalar-valued case. Let $\bar{\Theta} \in \mathcal{A}$. Then,

$$\frac{d}{dt}d_\psi(\bar{\Theta} \parallel \hat{\Theta}(t)) = (\hat{\Theta} - \bar{\Theta}) : \left(-\frac{1}{m} \sum_{i=1}^m \left(\mathbf{u}(\hat{\Theta}\alpha(\mathbf{x}_i)) - \mathbf{y}_i \right) \alpha^T(\mathbf{x}_i) \right)$$

Note that for two matrices $\mathbf{A}, \mathbf{B} \in \mathbb{R}^{n \times p}$ we have the equality $\mathbf{A} : \mathbf{B} = \text{Tr}(\mathbf{A}^T \mathbf{B})$. Hence,

$$\begin{aligned}
&= \text{Tr} \left[\left(\hat{\Theta} - \bar{\Theta} \right)^T \left(-\frac{1}{m} \sum_{i=1}^m \left(\mathbf{u} \left(\hat{\Theta} \alpha(\mathbf{x}_i) \right) - \mathbf{y}_i \right) \alpha^T(\mathbf{x}_i) \right) \right] \\
&= \text{Tr} \left[\left(-\frac{1}{m} \sum_{i=1}^m \left(\mathbf{u} \left(\hat{\Theta} \alpha(\mathbf{x}_i) \right) - \mathbf{y}_i \right) \alpha^T(\mathbf{x}_i) \right) \left(\hat{\Theta} - \bar{\Theta} \right)^T \right] \\
&= -\frac{1}{m} \sum_{i=1}^m \text{Tr} \left[\left(\mathbf{u} \left(\hat{\Theta} \alpha(\mathbf{x}_i) \right) - \mathbf{y}_i \right) \alpha^T(\mathbf{x}_i) \left(\hat{\Theta} - \bar{\Theta} \right)^T \right] \\
&= -\frac{1}{m} \sum_{i=1}^m \text{Tr} \left[\left(\mathbf{u} \left(\hat{\Theta} \alpha(\mathbf{x}_i) \right) - \mathbf{y}_i \right) \left(\left(\hat{\Theta} - \bar{\Theta} \right) \alpha(\mathbf{x}_i) \right)^T \right] \\
&= -\frac{1}{m} \sum_{i=1}^m \text{Tr} \left[\left(\mathbf{u} \left(\hat{\Theta} \alpha(\mathbf{x}_i) \right) - \mathbf{y}_i \right) \left(\hat{\Theta} \alpha(\mathbf{x}_i) - \mathbf{u}^{-1}(\mathbf{y}_i) \right)^T \right] \\
&= -\frac{1}{m} \sum_{i=1}^m \left(\mathbf{u} \left(\hat{\Theta} \alpha(\mathbf{x}_i) \right) - \mathbf{y}_i \right)^T \left(\hat{\Theta} \alpha(\mathbf{x}_i) - \mathbf{u}^{-1}(\mathbf{y}_i) \right)
\end{aligned}$$

In the derivation above, we have replaced $\bar{\Theta} \alpha(\mathbf{x}_i)$ by $\mathbf{u}^{-1}(\mathbf{y}_i)$ following our assumptions that $\bar{\Theta} \in \mathcal{A}$ and that \mathbf{u} is invertible. Integrating both sides of the above from 0 to ∞ , we find that

$$d_\psi \left(\bar{\Theta} \parallel \hat{\Theta}_\infty \right) = d_\psi \left(\bar{\Theta} \parallel \hat{\Theta}(0) \right) - \frac{1}{m} \sum_{i=1}^m \int_0^\infty \left(\mathbf{u} \left(\hat{\Theta}(t) \alpha(\mathbf{x}_i) \right) - \mathbf{y}_i \right)^T \left(\hat{\Theta}(t) \alpha(\mathbf{x}_i) - \mathbf{u}^{-1}(\mathbf{y}_i) \right) dt$$

The above relation is true for any $\bar{\Theta} \in \mathcal{A}$. Furthermore, the integral on the right-hand side is independent of $\bar{\Theta}$. Hence the arg min of the two Bregman divergences must be equal, which shows that

$$\hat{\Theta}_\infty = \arg \min_{\bar{\Theta} \in \mathcal{A}} d_\psi \left(\bar{\Theta} \parallel \hat{\Theta}(0) \right)$$

Initializing $\hat{\Theta}(0) = \arg \min_{\mathbf{W} \in \mathbb{R}^d} \psi(\mathbf{W})$ completes the proof. \square

By leveraging a recent contraction inequality for vector-valued output classes (Maurer, 2016), we can strengthen the guarantees of Theorem 4.2 without weight sharing by lowering the dependence from $n^{3/2}$ to n .

Theorem D.2 (Statistical guarantees for the vector-valued Reflectron without weight sharing). *Suppose that $\{\mathbf{x}_i, \mathbf{y}_i\}_{i=1}^m$ are drawn i.i.d. from a distribution supported on $\mathcal{X} \times [0, 1]^n$ with $\mathbb{E}[\mathbf{y}|\mathbf{x}] = \mathbf{u}(\Theta \alpha(\mathbf{x}))$ for a known function $\mathbf{u}(\mathbf{x})$ and an unknown matrix of parameters $\Theta \in \mathbb{R}^{n \times p}$. Assume that $\mathbf{u}(\mathbf{x})_i = u_i(x_i)$ where each $u_i : \mathcal{X}_i \rightarrow [0, 1]$ is L_i -Lipschitz and nondecreasing in its argument. Assume that $\alpha : \mathcal{X} \rightarrow \mathbb{R}^p$ is a known finite-dimensional feature map with $\|\alpha(\mathbf{x})\|_2 \leq C$ for all $\mathbf{x} \in \mathcal{X}$ where $C > 0$ is a constant. Let $d_\psi(\Theta \parallel \mathbf{0}) \leq \frac{\sigma}{2} W^2$ where ψ is σ -strongly convex with respect to $\|\cdot\|_F$ and $W > 0$ is a constant. Then, for any $\delta \in (0, 1)$, with probability at least $1 - \delta$ over the draws of $(\mathbf{x}_i, \mathbf{y}_i)$, there exists some time $t < \mathcal{O} \left(\frac{\sigma W}{C \sqrt{n}} \sqrt{m / \log(1/\delta)} \right)$ such that the hypothesis $\mathbf{h}_t(\mathbf{x}) = \mathbf{u} \left(\hat{\Theta}(t) \alpha(\mathbf{x}) \right)$ satisfies*

$$\begin{aligned}
\tilde{\varepsilon}(\mathbf{h}_t) &\leq \mathcal{O} \left(\frac{\max_k \{L_k\} C W}{\sqrt{m}} \sqrt{n \log(1/\delta)} \right), \\
\varepsilon(\mathbf{h}_t) &\leq \mathcal{O} \left(\frac{\max_k \{L_k\} C W}{\sqrt{m}} \left(n + \sqrt{n \log(1/\delta)} \right) \right),
\end{aligned}$$

where $\hat{\Theta}(t)$ is output by the Reflectron at time t with $\hat{\Theta}(0) = \mathbf{0}$.

Proof. Consider the rate of change of the Bregman divergence between the parameters for the Bayes-optimal predictor and the parameters produced by the Reflectron at time t ,

$$\frac{d}{dt} d_\psi \left(\Theta \parallel \hat{\Theta} \right) = \left(\hat{\Theta} - \Theta \right) : \nabla^2 \psi(\hat{\Theta}) : \dot{\hat{\Theta}}.$$

Following the proofs of Lemma D.1 and Theorem 3.1, we immediately have the inequality

$$\frac{d}{dt} d_\psi(\Theta \parallel \hat{\Theta}) \leq -\frac{1}{\max_k \{L_k\}} \varepsilon(\mathbf{h}_t) + \frac{1}{m} (\hat{\Theta} - \Theta) : \left(\sum_{i=1}^m (\mathbf{y}_i - \mathbf{u}(\Theta \alpha(\mathbf{x}_i))) \alpha^T(\mathbf{x}_i) \right)$$

Now, note that each $\frac{1}{C\sqrt{n}} (\mathbf{y}_i - \mathbf{u}(\Theta \alpha(\mathbf{x}_i))) \alpha^T(\mathbf{x}_i)$ is a zero-mean i.i.d. random variable with Frobenius norm bounded by 1 almost surely. Then, by Lemma C.1, $\left\| \frac{1}{C\sqrt{nm}} \sum_{i=1}^m (\mathbf{y}_i - \mathbf{u}(\Theta \alpha(\mathbf{x}_i))) \alpha^T(\mathbf{x}_i) \right\|_F \leq \eta$ with probability at least $1 - \delta$ where $\eta = \frac{2(1+\sqrt{\log(1/\delta)/2})}{\sqrt{m}}$. Assuming that $\|\hat{\Theta}(t) - \Theta\|_F \leq W$ at time t , we conclude that

$$\frac{d}{dt} d_\psi(\Theta \parallel \hat{\Theta}) \leq -\frac{1}{\max_k \{L_k\}} \hat{\varepsilon}(\mathbf{h}_t) + \sqrt{n}CW\eta.$$

Hence, either $\frac{d}{dt} d_\psi(\Theta \parallel \hat{\Theta}) < -\sqrt{n}CW\eta$, or $\hat{\varepsilon}(\mathbf{h}_t) \leq 2(\max_k \{L_k\}) \sqrt{n}CW\eta$. In the latter case, our result is proven. In the former, by our assumptions $d_\psi(\Theta \parallel \mathbf{0}) = d_\psi(\Theta \parallel \hat{\Theta}(0)) \leq \frac{\sigma}{2}W^2$, and hence $\|\hat{\Theta}(0) - \Theta\| \leq W$ by σ -strong convexity of ψ with respect to $\|\cdot\|_F$. Furthermore, $\|\hat{\Theta}(t) - \Theta\| \leq \sqrt{\frac{2}{\sigma} d_\psi(\Theta \parallel \hat{\Theta}(t))} \leq \sqrt{\frac{2}{\sigma} d_\psi(\Theta \parallel \hat{\Theta}(0))} \leq W$. Thus it can be until at most

$$t_f = \frac{d_\psi(\Theta \parallel \hat{\Theta}(0))}{\sqrt{n}CW\eta} = \frac{\sigma/2W^2}{\sqrt{n}CW\eta} = \frac{\sigma W}{2\sqrt{n}C\eta}$$

until $\hat{\varepsilon}(\mathbf{h}_t) \leq 2 \max_k \{L_k\} \sqrt{n}CW\eta$. Hence there is some \mathbf{h}_t with $t < t_f$ such that

$$\hat{\varepsilon}(\mathbf{h}_t) \leq \mathcal{O} \left(\sqrt{n} \max_k \{L_k\} CW \sqrt{\frac{\log(1/\delta)}{m}} \right).$$

Note that $\mathbf{u}(\cdot)$ is Lipschitz with constant $\max_k \{L_k\}$. Let $l_{\mathbf{y}}(\hat{\mathbf{y}}) = \|\hat{\mathbf{y}} - \mathbf{y}\|^2$ denote the square loss on example \mathbf{y} . Then $l_{\mathbf{y}} \circ \mathbf{u} : \mathbb{R}^n \rightarrow \mathbb{R}$ is $\sqrt{n} \max_k \{L_k\}$ Lipschitz and \sqrt{n} -bounded over the domain $[0, 1]^n$. We want to bound $\varepsilon(\mathbf{h}_t) - \hat{\varepsilon}(\mathbf{h}_t)$, which can be performed via

$$\begin{aligned} \sup_{\mathbf{f} \in \mathcal{F}} \left[\mathbb{E}_{\mathbf{X}} [(l_{\mathbf{y}} \circ \mathbf{u})(\mathbf{f}(\mathbf{X}))] - \frac{1}{m} \sum_{i=1}^m (l_{\mathbf{y}} \circ \mathbf{u})(\mathbf{f}(\mathbf{x}_i)) \right] \\ \leq \mathcal{O} \left(\mathbb{E}_{\mathbf{x}_i, \epsilon_i} \left[\sup_{\mathbf{f} \in \mathcal{F}} \frac{1}{m} \sum_{i=1}^m \epsilon_i (l_{\mathbf{y}} \circ \mathbf{u})(\mathbf{f}(\mathbf{x}_i)) \right] \right) + \mathcal{O} \left(\sqrt{\frac{n \log(1/\delta)}{m}} \right) \end{aligned}$$

with probability at least $1 - \delta$, where $\mathcal{F} = \{\hat{\Theta} \alpha(\mathbf{x}) : \|\hat{\Theta}\| \leq 2W, \|\alpha(\mathbf{x})\| \leq C\}$ and the ϵ_i are Rademacher random variables (Wainwright, 2019). Application of Theorem C.4 to bound the first term on the right-hand side above gives the bound

$$\varepsilon(\mathbf{h}_t) \leq \hat{\varepsilon}(\mathbf{h}_t) + \mathcal{O} \left(\frac{\max_k \{L_k\} CW n}{\sqrt{m}} \right) + \mathcal{O} \left(\sqrt{\frac{n \log(1/\delta)}{m}} \right)$$

which completes the proof. \square